Title

Genomic and transcriptomic mediators of resistance and response to antibody-drug conjugates (ADCs) in metastatic breast cancer (MBC)

Author

Alkassis, Samer

Publication Date

2025

Peer reviewed|Thesis/dissertation

UNIVERSITY OF CALIFORNIA

Los Angeles

Genomic and transcriptomic mediators of resistance and response to antibody-drug conjugates (ADCs) in metastatic breast cancer (MBC)

A dissertation submitted in partial satisfaction of the

requirements for the degree Master of Science

in Clinical Research

by

Samer Alkassis

2025

ABSTRACT OF THE THESIS

Genomic and transcriptomic mediators of resistance and response to antibody-drug conjugates (ADCs) in metastatic breast cancer (MBC)

by

Samer Alkassis

Master of Science in Clinical Research

University of California, Los Angeles, 2025

Professor Marc A. Suchard, Chair

Antibody-drug conjugates (ADCs) have transformed the treatment landscape for metastatic breast cancer (MBC), demonstrating significant efficacy. However, the emergence of resistance remains a substantial challenge, limiting their long-term effectiveness. This study investigates genomic and transcriptomic alterations associated with primary and acquired resistance to sacituzumab govitecan (SG), trastuzumab deruxtecan (T-DXd), and trastuzumab emtansine (T-DM1) using next-generation sequencing (NGS) data from the Tempus database. Non-paired pre- and post-treatment biopsies were analyzed to identify biomarkers of resistance, while correlations between pre-treatment profile and clinical response were assessed. High expression of drug efflux pump genes was significantly associated with shorter duration of treatment for patients receiving T-DXd and SG. Additionally, ERBB2 overexpression was linked to improved OS in the T-DXd group. Notably, no significant genomic or transcriptomic markers of resistance were identified for T-DM1. These findings enhance the understanding of molecular mechanisms

underlying ADC resistance, highlighting potential predictive biomarkers and therapeutic targets. Future investigations are warranted to validate these results and explore strategies to overcome resistance, ultimately informing personalized treatment approaches in MBC.

The dissertation of Samer Alkassis is approved.

Aditya Bardia

John A. Glaspy

David Elashoff

Marc A. Suchard, Committee Chair

University of California, Los Angeles

2025

TABLE OF CONTENTS

LIST OF TABLES AND FIGURES

ACKNOLEDGMENTS

This work is a version of the following manuscript draft currently in preparation for publication:

Alkassis S, Lipsyc-Sharf M, Traverso C, Mercer J, Yilma B, Fragkogianni S, Yuan Y, Meric-Bernstam F, Rugo H, O'Shaughnessy J, Rimawi M, Schiff R, Elashoff D, Glaspy J, McDermott M, Cummings A, Chao C, Aditya B

This work was funded by Tempus AI Inc.

Author Contribution:

S.A., J.G., C.C., and A.B. contributed substantially to the conception and design of the work. S.A., C.T., J.M., B.Y., S.F., and A.B. contributed to data acquisition, analysis, and interpretation. S.A., and A.B. drafted the manuscript. M.L.S., Y.Y., F.M.B., H.R., J.O., M.R., R.S., J.G., M.M., A.C., and A.B. contributed substantially to manuscript revision.

INTRODUCTION

Antibody-drug conjugates (ADCs) have revolutionized the therapeutic landscape in clinical oncology. Three components shape the structure of ADC—a monoclonal antibody, a cytotoxic payload, and a chemical linker that conjugates them. By combining the targeting precision of antibody with the potent cytotoxicity of the payload, ADCs are designed to enhance therapeutic efficacy while minimizing off-target effects and preserving normal tissue integrity. Four ADCs have been FDA-approved for metastatic breast cancer (MBC)—trastuzumab deruxtecan (T-DXd)[1] and trastuzumab emtansine (T-DM1)[2], both targeting HER2, and sacituzumab govitecan (SG)[3] and datopotamab deruxtecan (Dato-DXd)[4], targeting Trop-2 antigen. While T-DXd, Dato-DXd, and SG target topoisomerase I (TOP1) with their payloads[5,6], T-DM1 uses monomethyl auristatin E (MMAE), which inhibits tubulin polymerization, leading to cell cycle arrest and apoptosis[7]. Additionally, several other ADCs are currently in development. As research progresses in understanding the mechanisms and clinical applications of ADCs, these therapies have improved clinical outcomes in breast cancer, offering new therapeutic approaches for this complex disease. However, despite these advancements, most patients with MBC treated with ADCs ultimately have disease progression due to resistance, the underlying mechanisms of which are not yet fully understood.

Therapeutic resistance to ADCs can be classified as primary (*de novo*), where therapeutic efficacy is absent from the onset, and acquired, where an initial response is followed by subsequent treatment failure[8]. Conceptually, resistance can occur at multiple stages of the ADC pathway, including antigen binding, internalization, lysosomal degradation, and/or payload delivery[9,10]. Several potential mechanisms have been identified in breast cancer cell lines resistant to T-DM1, including instability and decreased expression of HER2, as well as reduced

binding and internalization of the antibody[11,12]. Upregulation of drug efflux pumps, including multidrug-resistant proteins (MRP1, MRP2, MDR1), has also been implicated in T-DM1 resistance, interfering with payload delivery[13–15]. Specific mutations in TOP1 gene have been observed in a patient with triple-negative breast cancer (TNBC) who experienced disease progression on SG[16]. Similarly, a loss-of-function mutation in SLX4, a key protein involved in DNA damage repair, was identified in a patient treated with T-DXd, both pre- and post-treatment[17]. While these mechanisms of resistance have been studied pre-clinically or in small cohorts of patients, comprehensive large-scale studies have not yet been conducted to investigate genomic alterations associated with resistance to ADCs, thereby limiting our understanding of the underlying mechanisms involved. Characterizing these alterations will provide valuable insight for potentially predicting biomarkers of resistance and developing therapeutic approaches to address this challenge.

Next generation sequencing (NGS) is increasingly applied in clinical practice to identify actionable molecular alterations in MBC[18]. Tempus is a leading technology company dedicated to advancing precision medicine through the integration of artificial intelligence (AI) and advanced data analytics. The company specializes in the collection and analysis of clinical and molecular data, including genomic sequencing and transcriptomic profiling, to inform personalized treatment strategies for patients with cancer. Through Tempus database, we retrospectively analyzed genomic and transcriptomic differences in patients with MBC who had biopsies before and after treatment with ADC (ADC_{tx}). In addition, we characterized the transcriptomic profile from patients who had biopsies prior to ADC_{tx} initiation to elucidate biomarkers of response to SG, T-DXd, and T-DM1.

METHODS

Study population:

De-identified records of patients with a primary diagnosis of breast cancer were identified through the Tempus Database (Tempus AI, Inc., Chicago, IL) and filtered to those who underwent Tempus xT next-generation sequencing (NGS). Patients were further selected based on stage IV disease documentation (within 60 days of biopsy) to identify patients with MBC **(Figure 1)**.

Treatment Groups:

Further selection was based on documented administration of any of the following ADC treatments: sacituzumab govitecan (SG), trastuzumab deruxtecan (T-DXd), or trastuzumab emtansine (T-DM1). The samples were split into **pre-treatment** (collected within 1 year before or 15 days after the ADC start date) or **post-treatment** (collected within 3 months after end of ADCtx or within 1 year of ADCtx initiation "if ADC end date is unknown") groups. Additionally, patients were subcategorized into those who received ADC for < 3 months versus > 3 months to distinguish between acquired and primary resistance, respectively. The cohort was split into three subsets based on resistance evaluation:

1) **Baseline profile:** pre-treatment samples from patients who did not exhibit primary resistance (treated with ADC for >3 months).
2) **Primary resistance (PrRes):** pre- and post-treatment samples from patients treated with ADC for 0-3 months.
3) **Acquired resistance (AcqRes):** post-treatment samples from patients treated with ADC for > 3 months.

Genomic Profiling:

NGS was conducted using the Tempus xT assay (Tempus AI, Inc., Chicago, IL), as previously described[19–21]. Briefly, Tempus xT is a targeted, tumor-normal-matched DNA panel that detects single-nucleotide variants, insertions and/or deletions, and copy number variants in 648 genes, as well as chromosomal rearrangements in 22 genes with high sensitivity and specificity. For RNA analysis, the Tempus xR assay was employed. Briefly, Tempus xR is a whole-transcriptome NGS assay spanning a 39 Mb target region of the human genome that quantifies transcript- and gene-level expression and identifies transcriptional evidence of chromosomal rearrangements resulting in the expression of fusion RNA species[22,23].

Variable Definition:

Demographic and clinical characteristics were compared between the pre-tx and post-tx groups. Demographic data included age, race, and ethnicity, while clinical characteristics encompassed tumor site and histology. Sample metadata, including the timing of sample collection relative to diagnosis, were also documented. The somatic and germline landscapes were characterized. Somatic alterations included pathogenic/likely pathogenic short variant mutations and copy number alterations, defined as copy number loss (0) or amplification (≥ 8). Germline alterations were considered only for patients with matched tumor-normal samples.

Acquired resistance was assessed by comparing non-matched pre-tx and post-tx biopsies in patients treated with ADCs for > 3 months. Primary resistance was analyzed by comparing pre- or post-tx biopsies from patients treated with ADC for ≤ 3 months and pre-tx biopsies from patients treated with ADC for > 3 months.

Statistical Analyses:

Continuous and categorical demographic variables were compared using the Wilcoxon rank-sum test and Fisher's exact test, respectively. Somatic differences between groups were evaluated using Pearson's Chi-squared test or Fisher's exact test, as appropriate. The median log2(TPM) gene expression was compared between groups using the Wilcoxon rank-sum exact test. For biomarker analysis, the correlation between treatment duration (DoT) and gene expression was assessed using Pearson's correlation coefficient.

Cox proportional hazards models with risk-set adjustment were employed to test associations between pre-treatment gene expression and overall survival (OS), with gene expression modeled as a continuous linear predictor. The proportional hazards assumption of the Cox proportional hazards models were checked by fitting each gene expression measure as a time-varying coefficient and investigating the resulting residual plots. If evidence of non-proportionality was detected, then this suggests that the effect of the gene expression measure on OS is non-constant over time and a point estimate is inadequate to summarize the relationship with OS. In these situations, the Cox modeling results were excluded. Since the gene expression measures were included as continuous predictors in the Cox proportional hazards models for OS and were assumed to have linear associations with OS, the linearity of these effects on OS were tested by also modeling the effect using linear-tail-restricted natural splines with 4 knots which makes fewer assumptions to the functional form of the relationship. If the spline-based estimates were found to add significant predictive ability to the OS model over and above the linear term, then this would suggest that the effect of the gene expression measure on OS is non-linear. Nominal statistical significance was set at $p < 0.05$. The Benjamini and Hochberg approach to controlling the False Discovery Rate (FDR) was performed for some analyses. This approach uses the

unadjusted p-values to generate q-values that control the FDR across a defined set of statistical tests. This correction was applied to the results of the Pearson's Chi-squared and Fisher's exact tests from the somatic landscape analyses and, separately, to the results of Wilcoxon rank-sum exact tests from the comparisons of median log2(TPM + 1) gene expression levels. No sort of correction was applied to the Pearson's correlation coefficient analyses for the correlations between gene expression and duration of treatment or the gene expression and OS analyses due to smaller number of comparisons.

RESULTS

Patients' characteristics and biopsy information:

T-DXd Groups:

A total of 202 patients were included in the pre-tx cohort (pre-T-DXd$_{tx}$) and 39 in the post-treatment cohort (post-T-DXd$_{tx}$) **(Table 1a)**. The median age at primary diagnosis was 53 years in the pre-T-DXd$_{tx}$ group and 51 years in the post-T-DXd$_{tx}$ group, while the median age at metastatic diagnosis was 60 and 57 years, respectively. Race distribution differed significantly (p = 0.031), with a higher proportion of white patients in the pre-T-DXd$_{tx}$ group (53% vs. 49%). Ethnicity distributions were comparable, with most patients in both groups being non-Hispanic or Latino. Hormone receptor (HR) status was similar between groups, with HR+/HER2- breast cancer being the most common subtype (41% pre-T-DXd$_{tx}$ vs. 44% post-T-DXd$_{tx}$). The post-T-DXd$_{tx}$ cohort had a higher proportion of breast cancer classified as not otherwise specified (NOS) (33% vs. 18%), while the pre-T-DXd$_{tx}$ group had more cases of triple-negative breast cancer (TNBC) (16% vs. 10%). HR+/HER2+ and HR-/HER2+ subtypes were less frequent in the post-T-DXd$_{tx}$ group. The median duration of ADC therapy was longer in the post-T-DXd$_{tx}$ group

(218 vs. 163 days). Sample collection occurred at a median of 3 months before ADC initiation in the pre-T-DXd$_{tx}$ group (IQR: -8 to -1 months) and 3 months after ADC discontinuation in the post-T-DXd$_{tx}$ group (IQR: 1 - 4 months). Missing data were noted in the pre-T-DXd$_{tx}$ group for ADC duration and sample collection timing.

SG Groups:

The pre-treatment cohort (pre-SG$_{tx}$) consisted of 243 patients while the post-treatment cohort (post-SG$_{tx}$) included 49 participants **(Table 1b)**. The median age at primary diagnosis was 51 years in both groups, while the median age at metastatic diagnosis was 55 years in the pre-SGtx group and 57 years in the post-SG$_{tx}$ group. Racial and ethnic distributions were comparable in both groups. HR status distribution differed significantly ($p = 0.03$). TNBC was more prevalent in the pre-SG$_{tx}$ group (62% vs. 41%), whereas the post-SG$_{tx}$ group had a higher proportion of HR+/HER2- (27% vs. 20%) and breast cancer NOS (33% vs. 17%). The median ADC duration was longer in the post-SGtx group than in the pre-SGtx group (178 vs. 120 days). Sample collection occurred at a median of 4 months before ADC initiation in the pre-SGtx cohort (IQR: -8 to -1 months) and 1 month after ADC discontinuation in the post-SGtx cohort (IQR: 1 - 3 months). Missing data were noted in the pre-SG$_{tx}$ group for ADC duration and biopsy timing relative to ADC end.

T-DM1 Groups:

A total of 84 patients were included in the pre-treatment cohort (pre-T-DM1$_{tx}$) and 23 in the post-treatment cohort (post-T-DM1$_{tx}$) **(Table 1c)**. The median age at primary diagnosis was 55 years in the pre-T-DM1$_{tx}$ group and 50 years in the post-T-DM1$_{tx}$ group, while the median age at

metastatic diagnosis was 59 and 55 years, respectively. Race and ethnicity distributions were similar between the cohorts. HR status distribution differed significantly ($p = 0.008$). HR+/HER2+ breast cancer was more common in the pre-T-DM1$_{tx}$ group (42% vs. 26%), as well as HR-/HER2+ disease (23% vs. 8.7%). The proportion of breast cancer classified as NOS was identical in both groups (26%). The median duration of ADC treatment in the pre-T-DM1$_{tx}$ group was 148 days vs. 169 days in the post-T-DM1$_{tx}$ group. Sample collection occurred at a median of 2 months before ADC initiation in the pre-T-DM1$_{tx}$ group (IQR: -6 to -0.9 months) and 1 month after ADC discontinuation in the post-T-DM1$_{tx}$ group (IQR: 0 – 3 months). Missing data were noted for ADC treatment duration and biopsy timing relative to ADC end in the pre-T-DM1$_{tx}$ group.

Biomarkers of therapeutic response:

A total of 453 patients with pre-tx biopsies ($N_{T\text{-}DXd} = 178$, $N_{SG} = 204$, $N_{T\text{-}DM1} = 71$) were included in the transcriptomic analysis **(Table 2)**. HR and HER2 status varied significantly ($p < 0.001$), with the highest proportion of HR+/HER2+ disease in the T-DM1 group (45%), while the SG group had the most TNBC cases (62%). Median DoT across all patients was 130 days (T-DXd: 144 days, SG: 116 days, T-DM1: 148 days).

A negative correlation was observed between drug efflux pump gene expression and DoT for T-DXd (ABCB1: r = -0.290, $p = 0.017$; ABCC1: r = -0.274, $p = 0.025$), with higher pre-tx gene expression associated with shorter DoT **(Table 3a, Figure 3a)**. Additionally, higher pre-tx expression of ABCB1 was associated with worse OS (HR: 1.30, 95% CI: 1.10 - 1.53, $p = 0.002$) **(Figure 4a)**. While no significant correlation was found between ERBB2 expression and DoT (r = 0.041, $p = 0.742$), a significant positive correlation was observed with OS (HR = 0.8, $p =$

0.018). TOP1 gene expression was not significantly correlated with shorter DoT or worse OS (r = 0.12, $p = 0.32$; HR = 1.67, $p = 0.13$) **(Figure 2a)**. Similarly, no significant correlation was observed with any of the DNA damage repair markers.

In the SG cohort, no association was found between TACSTD2 expression, encoding Trop-2, and DoT (r = -0.103, $p = 0.334$) **(Figure 2b)**. While no significant correlations between drug efflux pump expression and DoT were found **(Figure 3b)**, higher pre-tx ABCC1 and ABCC4 gene expressions were associated with worse OS (ABCC1: HR = 1.34, $p = 0.034$; ABCC4: HR= 1.19, $p = 0.042$) **(Figure 4b)**. TOP1 gene expression was not significantly correlated with shorter DoT or worse OS (r = 0.16, $p = 0.12$; HR = 0.73, $p = 0.16$). However, higher expression of PRKDC, a DNA damage repair protein gene, was linked to worse OS (HR: 1.37, $p = 0.008$), while EMSY expression was associated with better survival (HR: 0.608, $p = 0.004$). In the T-DM1 cohort, no significant associations were found between pre-tx efflux pump, TUBB1 or ERBB2 gene expression and DoT or OS **(Table 3b, Figures 2c, 3c, 4c)**. A broader transcriptomic analysis encompassing DNA damage repair genes, alternative signaling pathways, and compensatory survival mechanisms is presented in the **Extended data table 1**.

<u>Analysis of acquired resistance:</u>

Comparison between pre-tx (**Baseline**: $N_{T\text{-}DXd} = 67$, $N_{SG} = 64$, $N_{T\text{-}DM1} = 34$) and post-tx profiles (**AcqRes**: $N_{T\text{-}DXd} = 27$, $N_{SG} = 38$, $N_{T\text{-}DM1} = 10$) of patients with ADC duration > 3 months was conducted. No significant differences were observed in the incidence of ERBB2 mutation/ amplification or gene expression between pre- and post-T-DXd$_{tx}$ cohorts (alteration: 27% vs. 33%, $p = 0.5$; expression: 8.2 vs. 8.05, $p > 0.9$) **(Table 4a)**. A trend toward higher expression across efflux pump genes was seen in post-T-DXd $_{tx}$ group (ABCC1: 6.34 vs. 6.7, $p = 0.016$, q =

0.4; ABCB1: 2.77 vs. 3.44, $p = 0.4$) **(Figure 5)**. However, no significant differences were observed in TOP1 gene expression (6.92 vs. 6.96, $p = 0.8$) or SLX4 gene expression (4.81 vs. 5.06, $p = 0.3$).

In SG cohort **(Table 4b)**, no significant difference was demonstrated in the expression of TACSTD2 (7.49 vs. 7.75, $p = 0.8$), TOP1 (7.04 vs. 6.97, $p = 0.4$), or SLX4 genes (4.56 vs. 4.51, $p = 0.4$). However, a trend toward higher expression across efflux pump genes was seen in post-SG_{tx} (ABCB1: 2.66 vs 3.4, $p = 0.07$, q = 0.8; ABCC2: 2.4 vs 3.4, $p = 0.2$) **(Figure 5)**.

Compared to pre-$T\text{-}DM1_{tx}$ group **(Table 4c)**, there was a decrease in the incidence of ERBB2 alterations (69% vs 40%, $p = 0.047$, q > 0.9) as well as a decrease in gene expression (10.91 vs. 8.44, $p = 0.024$, q = 0.3) in post-$T\text{-}DM1_{tx}$ cohort **(Figure 6)**. No mutations were observed in ABCC3 gene in post-$T\text{-}DM1_{tx}$ group. However, mixed changes across efflux pump genes expression were demonstrated (ABCB1: 3.3 vs. 2.7, $p = 0.08$, q = 0.4; ABCC1: 6.3 vs. 6.8, $p = 0.05$, q = 0.3; ABCC2: 3.19 vs. 3.18, $p = 0.2$) **(Figure 5)**. A broader somatic and transcriptomic analyses are presented in the **Extended data table 2a-c**.

Analysis of primary resistance:

We compared pre- or post-tx profile for patients with ADC duration $\leq$ 3 months (**PrRes:** $N_{T\text{-}DXd} = 26$, $N_{SG} = 55$, $N_{T\text{-}DM1} = 27$) with pre-tx profile of patients with ADC duration > 3 months (**Baseline:** $N_{T\text{-}DXd} = 67$, $N_{SG} = 64$, $N_{T\text{-}DM1} = 42$). In the T-DXd cohort there was no difference in the incidence of ERBB2 alteration between PrRes vs. baseline cohorts (15% vs. 27%, $p = 0.2$) **(Extended data table 1)**. However, a trend of lower ERBB2 expression was observed in patients with an ADC duration $\leq$ 3 months (7.81 vs. 8.19, $p = 0.062$). No significant difference in drug efflux pump gene expression was demonstrated between both groups (ABCC1: 6.38 vs. .34, $p =$

0.3; ABCC2: 2.64 vs. 3.25, $p = 0.6$; ABCB1: 3.18 vs. 2., $p = 0.074$). Mutation in TOP1 and ATM were identified in two distinct patients of the PrRes cohort.

Although not statistically significant, there was a trend indicating higher efflux pump gene expression associated with primary resistance to SG (ABCB1: 2.84 vs. 2.66, $p = 0.6$; ABCC2: 2.96 vs. 2.44, $p = 0.7$). Overall, there were no significant differences in mutation or expression of genes associated with ADC processing or DNA damage repair, though **(Extended data table 2)**. In the T-DM1 group, the incidence of ERBB2 mutation/amplification was observed to be lower in patients with an ADC duration ≤ 3 months, although this difference did not reach statistical significance (48% vs. 69%, $p = 0.08$) **(Extended data table 3)**. However, a decrease in ERBB2 expression was correlated with primary resistance (8.76 vs. 10.91, $p = 0.02$, q = 0.4). There were no significant difference in drug efflux pump gene expression between both groups (ABCC1: 6.29 vs. 6.34, $p = 0.2$; ABCC2: 2.79 vs. 3.19, $p = 0.4$; ABCB1: 2.90 vs. 3.34, $p = 0.8$) (**Figure 7)**. A broader somatic and transcriptomic analyses are presented in the **Extended data table 3a-c**.

DISCUSSION

ADCs have emerged as a promising therapeutic strategy in clinical oncology, leading to notable improvement in clinical outcomes. However, the development of resistance to ADCs has posed a significant challenge, undermining their long-term efficacy. Resistance can emerge at multiple stages of the ADC pathway, highlighting the need for a deeper understanding of its multifactorial mechanisms. In this study, we explored potential mediators to both primary and acquired resistance by focusing on three critical components of the ADC pathway—antigen-related factors, payload target interaction, and the role of drug efflux pumps.

Antibody-Antigen binding is the key to identify the cancer cells. In the phase II trial of T-DM1, higher antigen expression correlated with improved response rates[24]. Decreased HER2 expression in cancer cell lines was observed upon exposure to trastuzumab-maytansinoid ADC[14] which was demonstrated in one of the T-DM1-resistant models developed by Li et al[15]. Similarly, in TNBC, primary resistance to SG was linked to the lack of TROP2 expression in one patient[16]. Notably, our analysis of acquired resistance in patients treated with T-DM1 revealed a decrease in ERBB2 expression in the post-treatment cohort compared to the pre-treatment group. This trend was not seen in the T-DXd cohorts, which is consistent with T-DXd's proven efficacy in HER2-low and ultra-low disease. In our primary resistance analysis, a decrease in ERBB2 expression significantly correlated with resistance to T-DM1, and a trend toward lower ERBB2 expression was noted in patients with T-DXd treatment duration $\leq$ 3 months.

In addition to decreased expression, HER2-related resistance in breast cancer can be secondary to HER2 instability, heterogeneity, or impaired binding[12]. Intratumoral HER2 heterogeneity is reported in up to 40% in breast cancer[25–30], more commonly in equivocal HER2 expression[31], with a negative impact on response to ADC. In the KRISTINE trial, patients with intra-tumoral heterogeneity showed no pathologic complete response to neoadjuvant T-DM1 plus pertuzumab[32,33]. Acquired resistance to SG was also observed due to missense mutation in TACSTD2 leading to decreased TROP2 expression[16]; however, this was not seen in our study.

Payload-related resistance can arise from specific mutations in cytotoxic targets or the upregulation of drug efflux pumps. Alterations in the microtubule/tubulin complex have been described in T-DM1-resistant cell line[34]. For topoisomerase inhibitor-based ADCs—including SG and T-DXd—resistance can occur through modifications in target expression or alterations in downstream signaling pathways[35]. Four distinct TOP1 mutations were identified in

topoisomerase inhibitor-based ADCs, representing the first report of TOP1 mutations emerging under selective pressure and their contribution to cross-resistance to subsequent ADCs with the same payloads[36,37]. Similarly, specific mutations in the TOP1 gene were identified in patients with TNBC who experienced disease progression on SG treatment[16]. These findings highlight the potential of TOP1 mutation as a biomarker of resistance in this context. Apart from TOP1 mutations, DNA damage repair (DDR) pathways can play a pivotal role in mediating resistance to HER2-based ADC[38]. Loss-of-function mutation in SLX4, a key DDR protein, was identified as a potential mechanism of resistance to T-DXd in the DAISY trial[39,40]. This was also demonstrated with SG, where the proficiency of the homologous recombination repair pathway compensates for DNA damage induced by its active payload, SN-38[41]. Our study did not detect significant changes in TOP1 or SLX4 gene expression in the post-T-DXd$_{tx}$ and post-SG$_{tx}$ cohorts, though mutations in TOP1 and ATM were identified in primary resistance cohorts of two distinct patients treated with T-DXd for $\leq$ 3 months.

The drug-to-antibody ratio (DAR) and the location of conjugations are crucial components influencing ADC efficacy. While the optimal drug-antibody ratio (DAR) remains unclear, Hamblett et al. demonstrated an optimal average of 2-4 for cysteine-conjugated ADCs and 3-4 for lysine-linked ADCs[42]. Preclinical studies have shown that high-DAR ADCs exhibit more rapid clearance and reduced efficacy[43], although other factors, including the site of conjugation and drug loading, may also contribute to these outcomes[10]. In one study comparing ADCs with the same antibody and payload, lysine-linked ADCs showed improved efficacy over cysteine-linked ADCs[44]. Conversely, in another study using a different payload, the opposite result was observed, further emphasizing the fact that conjugation chemistry must be assessed in the context of the specific antibody, target, and payload[45].

The export of cytotoxic agents from the cellular cytosol due to overexpression of drug efflux pumps is a well-characterized mechanism of resistance to conventional chemotherapies[46]. Several payloads are substrates for ATP-binding cassette (ABC) transporters, which are implicated in the development of multi-drug resistant (MDR) phenotypes[47–49]. In T-DM1-resistant cell lines, higher expression of MDR-associated proteins, such as MRP1 (encoded by ABCC1) and MRP2 (encoded by ABCC2), was also observed. Interestingly, inhibition of these proteins could restore sensitivity to T-DM1[14,15,50]. This observation was extended in an SG-resistant breast cancer cell line, where overexpression of the breast cancer resistance protein (BCRP), encoded by ABCG2, was detected [48]. Additionally, a recent multi-omic molecular profiling study identified ABCC1 expression as the most significant negative predictor of both time on treatment and OS in patients treated with T-DXd[51]. Our findings align with previous reports, demonstrating a trend toward increased expression of efflux pump genes in the post-T-DXd_{tx} (ABCB1, ABCC1) and in the post- SG_{tx} groups (ABCB1, ABCC2), as key contributors to acquired resistance. Mixed changes in the expression of efflux pump genes were also observed in the post-T-$DM1_{tx}$ cohort (ABCB1, ABCC1, ABCC2). Interestingly, in the primary resistance cohorts, increased ABCB1 expression was observed in the T-DXd group for patients treated for $\leq$ 3 months. Among the efflux pump genes evaluated, ABCB1 appeared to be the most relevant in the context of treatment response and secondarily ABCC1. Notably, in the case of T-DM1, which contains MMAE, no significant association with these efflux pumps was observed—unlike what was seen with SG or T-DXd. However, it is important to note that the sample size for the T-DM1 group was limited compared to other groups.

The identification of predictive biomarkers for ADC response has become a priority in clinical research. Genomic analysis of DDR gene variants, in the TROPiCS-02 study, revealed that 58%

of tumors had deleterious DDR alterations, with BRCA2, PRKDC, and ATM being most common[52]. While SG was more effective than physician's choice treatment in both DDR wild-type and mutant tumors, patients with DDR-deficient tumors experienced a greater benefit suggesting a potential synergy between DDR defects and SG's anti-tumor effects[52]. This was also observed in the exploratory biomarker analysis of T-DXd from the DESTINY-Breast04 trial, which found that BRCA1/2 or homologous recombination repair alterations, along with higher expression of DDR and cell proliferation gene signatures, were associated with shorter PFS. In patients treated with T-DM1, RAB5A, a protein involved in endocytic trafficking, has been identified as a potential predictive biomarker for treatment response, as confirmed in subsets of patients treated with T-DM1/pertuzumab in the I-SPY2 and KAMILLA trials[53]. Our findings highlight that the expression of drug efflux genes is significantly associated with response in both the T-DXd and SG cohorts.

Our study leverages a robust genomic profiling strategy utilizing NGS panel to assess both DNA and RNA signatures in patients with MBC. By targeting key molecular drivers of resistance to ADCs, including antigen expression, efflux pumps, and payload targets, the research provides valuable insights into both primary and acquired resistance mechanisms to T-DXd, SG, and T-DM1. These findings have the potential to inform the development of predictive biomarkers, thereby advancing personalized therapeutic strategies in ADC field. However, several limitations warrant consideration. First, the lack of matched pre- and post-treatment biopsies limited the ability to accurately compare changes in the genomic profile and assess acquired resistance. Second, the retrospective nature of this analysis, encompassing patients who had previously received ADC therapy, introduces inherent constraints, including missing clinical data. This limitation restricts our ability to perform a fully comprehensive evaluation of treatment

responses, resistance dynamics, and long-term outcomes. Assessing intra-tumoral HER2 heterogeneity was not feasible due to the absence of biopsies from distinct tumor sites, which are necessary to account for this significant factor. Additionally, the precise reasons for ADC discontinuation—whether due to radiographic or clinical disease progression, treatment-related toxicities, or other clinical factors—were not systematically documented. This lack of standardized discontinuation criteria prevents a more granular assessment of whether resistance mechanisms differ between patients discontinuing therapy due to disease progression versus those stopping treatment secondary to adverse events. Furthermore, the relatively small sample size within each ADC treatment cohort limits the statistical power of our findings and precludes robust subgroup analyses stratified by molecular features or prior treatment exposures.

Our study population, who had access to Tempus NGS, represent a clinically selected subset with sufficient tissue for sequencing and care at centers equipped for molecular profiling. Consequently, they may not reflect the broader population with MBC, particularly those with limited tissue availability or barriers to testing. This introduces potential selection bias and limits the generalizability of the study findings, particularly with respect to demographic, clinical, and socioeconomic diversity. While our multi-modal analyses identified potential biomarkers of resistance, larger prospective studies with well-annotated clinical and molecular datasets are needed to validate these findings.

CONCLUSION

Our comprehensive genomic and transcriptomic analysis of patients with MBC treated with ADCs revealed key mechanisms underlying both primary and acquired resistance. Notably, increased expression of drug efflux pumps, was strongly associated with reduced drug efficacy.

This finding suggests a potential mechanistic link between ADC payload release, the bystander effect, and treatment resistance. Through multi-modal analyses, we identified efflux pump gene expression as a promising biomarker for predicting both primary response and resistance to ADC therapy. Additionally, heterogeneity in antigen expression and alterations in DNA damage response pathways emerged as potential contributors to treatment failure, underscoring the complexity of ADC resistance mechanisms. These insights highlight the need for further validation in larger patient cohorts and preclinical models. To overcome ADC resistance, therapeutic strategies targeting drug efflux mechanisms—such as efflux pump inhibitors or modified linker-payload designs—could enhance intracellular drug retention and efficacy. Moving forward, leveraging advanced technologies like single-cell RNA sequencing and spatial transcriptomics will be crucial in refining our understanding of these resistance pathways and guiding the development of next-generation ADCs. Ultimately, these efforts aim to improve treatment outcomes and durability of response in patients with MBC.

Characteristic	Pre-T-DXd$_{tx}$ N = 202	Post-T-DXd$_{tx}$ N = 39	p-value
Age at Primary Diagnosis — Years			0.10
Median (IQR)	53 (45, 64)	51 (41, 58)	
Unknown	18	6	
Age at Metastatic Diagnosis — Years			0.2
Median (IQR)	60 (51, 68)	57 (48, 65)	
Race — N (%)			0.03
White	107 (53%)	19 (49%)	
Unknown	44 (22%)	17 (44%)	
Black or African American	24 (12%)	1 (2.6%)	
Other Race	19 (9.4%)	1 (2.6%)	
Asian	8 (4.0%)	1 (2.6%)	
Ethnicity — N (%)			>0.9
Not Hispanic or Latino	99 (85%)	15 (83%)	
Hispanic or Latino	18 (15%)	3 (17%)	
Unknown	85	21	
Breast Cancer Subtype — N (%)			0.2
HR+, HER2-	82 (41%)	17 (44%)	
NOS	37 (18%)	13 (33%)	
TNBC	33 (16%)	4 (10%)	
HR+, HER2+	25 (12%)	3 (7.7%)	
HR-, HER2+	25 (12%)	2 (5.1%)	
ADC Tx Duration— Days			
Median (IQR)	163 (104, 245)	218 (80, 282)	
Unknown	124	1	
Duration from ADC Start Date to Sample Collection— Months			
Median (IQR)	-3 (-8, -1)	9 (5, 12)	
Unknown	0	1	
Duration from ADC End Date to Sample Collection— Months			
Median (IQR)	-11 (-13, -7)	3 (1, 4)	
Unknown	124	0	

Table 1a: Patients' characteristics and biopsy information (T-DXd)

Characteristic	Pre-SG$_{tx}$ N = 243	Post-SG$_{tx}$ N = 49	p-value

Age at Primary Diagnosis— Years			0.7
Median (IQR)	51 (43, 61)	51 (40, 57)	
Unknown	12	7	
Age at Metastatic Diagnosis— Years			0.5
Median (IQR)	55 (46, 64)	57 (47, 64)	
Race— N (%)			0.5
White	127 (52%)	24 (49%)	
Unknown	61 (25%)	18 (37%)	
Black or African American	40 (16%)	5 (10%)	
Other Race	10 (4.1%)	1 (2.0%)	
Asian	5 (2.1%)	1 (2.0%)	
Ethnicity— N (%)			>0.9
Not Hispanic or Latino	125 (89%)	18 (90%)	
Hispanic or Latino	16 (11%)	2 (10%)	
Unknown	102	29	
Breast Cancer Subtype— N (%)			0.03
TNBC	151 (62%)	20 (41%)	
HR+, HER2-	49 (20%)	13 (27%)	
NOS	41 (17%)	16 (33%)	
HR-, HER2+	1 (0.4%)	0 (0%)	
HR+, HER2+	1 (0.4%)	0 (0%)	
ADC Tx Duration— Days			
Median (IQR)	120 (65, 198)	178 (97, 246)	
Unknown	139	0	
Duration from ADC Start Date to Sample Collection— Months			
Median (IQR)	-4 (-8, -1)	8 (5, 11)	
Duration from ADC End Date to Sample Collection— Months			
Median (IQR)	-9 (-14, -6)	1 (1, 3)	
Unknown	139	0	

Table 1b: Patients' characteristics and biopsy information (SG)

Characteristic	**Pre-T-DM1$_{tx}$** N = 84	**Post-T-DM1$_{Tx}$** N = 23	**p-value**

Age at Primary Diagnosis— Years			0.08
Median (IQR)	55 (46, 63)	50 (41, 58)	
Unknown	8	3	
Age at Metastatic Diagnosis— Years			0.2
Median (IQR)	59 (48, 68)	55 (45, 65)	
Race— N (%)			0.14
White	49 (58%)	11 (48%)	
Unknown	23 (27%)	5 (22%)	
Black or African American	7 (8.3%)	4 (17%)	
Other Race	2 (2.4%)	3 (13%)	
Asian	3 (3.6%)	0 (0%)	
Ethnicity— N (%)			>0.9
Not Hispanic or Latino	39 (91%)	8 (100%)	
Hispanic or Latino	4 (9.3%)	0 (0%)	
Unknown	41	15	
Breast Cancer Subtype— N (%)			0.008
HR+, HER2+	35 (42%)	6 (26%)	
NOS	22 (26%)	6 (26%)	
HR-, HER2+	19 (23%)	2 (8.7%)	
HR+, HER2-	4 (4.8%)	7 (30%)	
TNBC	4 (4.8%)	2 (8.7%)	
ADC Tx Duration— Days			
Median (IQR)	148 (74, 303)	169 (68, 234)	
Unknown	23	1	
Duration from ADC Start Date to Sample Collection— Months			
Median (IQR)	-2.0 (-6.0, -0.9)	6.6 (4.0, 10.6)	
Unknown	0	1	
Duration from ADC End Date to Sample Collection— Months			
Median (IQR)	-9 (-13, -7)	1 (0, 3)	
Unknown	23	0	

Table 1c: Patients' characteristics and biopsy information (T-DM1)

Characteristic	**All Patients** N=453	**T-DM1** N=71	**T-DXd** N=178	**SG** N=204	**p-value**

Age at Primary Diagnosis— Years					0.10
Median (Q1, Q3)	52 (44, 63)	55 (46, 64)	54 (45, 64)	52 (43, 62)	
Missing Observations	30	5	14	11	
Gender— N (%)					0.04
Female	449 (99%)	69 (97%)	176 (99%)	204 (100%)	
Male	4 (0.9%)	2 (2.8%)	2 (1.1%)	0 (0%)	
Race— N (%)					0.52
Asian	9 (2.0%)	1 (1.4%)	5 (2.8%)	3 (1.5%)	
Black or African American	64 (14%)	7 (9.9%)	23 (13%)	34 (17%)	
Other Race	23 (5.1%)	2 (2.8%)	13 (7.3%)	8 (3.9%)	
Unknown	109 (24%)	22 (31%)	40 (22%)	47 (23%)	
White	248 (55%)	39 (55%)	97 (54%)	112 (55%)	
Ethnicity— N (%)					0.97
Not Hispanic or Latino	228 (88%)	32 (89%)	89 (88%)	107 (87%)	
Hispanic or Latino	32 (12%)	4 (11%)	12 (12%)	16 (13%)	
Missing Observations	193	35	77	81	
Breast Cancer Subtype— N (%)					<0.001
HR-, HER2+	37 (8.2%)	16 (23%)	20 (11%)	1 (0.5%)	
HR+, HER2-	122 (27%)	4 (5.6%)	78 (44%)	40 (20%)	
HR+, HER2+	50 (11%)	32 (45%)	17 (9.6%)	1 (0.5%)	
NOS	83 (18%)	15 (21%)	33 (19%)	35 (17%)	
TNBC	161 (36%)	4 (5.6%)	30 (17%)	127 (62%)	
ADC Tx Duration— Days					0.10
Median (Q1, Q3)	130 (76, 225)	148 (63, 306)	144 (103, 221)	116 (62, 198)	
Missing Observations	246	20	111	115	

Table 2: Patients' characteristics for biomarkers of response analysis

	T-DXd	SG	T-DM1

Gene	*r* (DoT)	HR (95% CI)	p-value	*r* (DoT)	HR (95% CI)	p-value	*r* (DoT)	HR (95% CI)	*p*
Antigen									
TACSTD2				-0.103	1.007 (0.900 - 1.127)	0.90			
ERBB2	0.041	**0.806 (0.674 - 0.963)**	**0.02**				0.128	0.790 (0.617 - 1.011)	0.06
Payload Target									
TUBB1							0.041	1.341 (0.837 - 2.146)	0.22
TOP1	0.124	1.668 (0.854 - 3.256)	0.13	0.164	0.731 (0.473 - 1.129)	0.16			
SLX4	0.062	1.147 (0.762 - 1.727)	0.51	-0.020	0.887 (0.617 - 1.276)	0.52			
PRKDC	-0.035	1.299 (0.889 - 1.898)	0.18	-0.030	**1.372 (1.086 - 1.733)**	**0.008**			
EMSY	-0.040	1.049 (0.764 - 1.441)	0.77	0.089	**0.608 (0.432 - 0.855)**	**0.004**			
Drug Efflux Pump									
ABCB1	**-0.290**	**1.296 (1.100 - 1.526)**	**0.002**	0.012	1.008 (0.873 - 1.165)	0.91	-0.045	1.071 (0.796 - 1.440)	0.65
ABCC1	-0.274	1.216 (0.837 - 1.767)	0.30	0.023	**1.337 (1.022 - 1.749)**	**0.03**	0.196	1.064 (0.568 - 1.994)	0.85
ABCC2	-0.101	1.091 (0.970 - 1.227)	0.15	-0.091	1.004 (0.896 - 1.125)	0.94	0.035		
ABCC3	-0.026	0.858 (0.707 - 1.041)	0.12	-0.089	1.080 (0.929 - 1.256)	0.32	0.233	1.097 (0.820 - 1.469)	0.53
ABCC4	-0.158	0.933 (0.777 - 1.119)	0.45	-0.135	**1.192 (1.007 - 1.412)**	**0.04**	-0.149	1.064 (0.783 - 1.446)	0.69
ABCG2	-0.120	1.214 (0.987 - 1.494)	0.07	0.053	0.953 (0.795 - 1.141)	0.6	-0.035	0.996 (0.709 - 1.399)	0.98

Table 3: Biomarkers of response, correlation with duration of treatment (DoT) and overall survival (OS). ***r***: Pearson's correlation coefficient

Somatic Profile				
Gene	**Baseline Pre-T-DXd$_{tx}$** N = 67	**AcqRes Post-T-DXd$_{tx}$** N = 27	**p-value**	**q-value**
ERBB2	18 (27%)	9 (33%)	0.5	>0.9
ABCC3	4 (6.0%)	1 (3.7%)	>0.9	>0.9
ATM	0 (0%)	1 (3.7%)	0.3	>0.9
BRCA1	1 (1.5%)	0 (0%)	>0.9	>0.9
BRCA2	0 (0%)	1 (3.7%)	0.3	>0.9
MSH6	0 (0%)	1 (3.7%)	0.3	>0.9
ATR	2 (3.0%)	0 (0%)	>0.9	>0.9
EMSY	2 (3.0%)	0 (0%)	>0.9	>0.9
CHEK2	1 (1.5%)	0 (0%)	>0.9	>0.9
Transcriptomic Profile				
Gene	**Baseline** N = 57[1]	**AcqRes** N = 13[1]	**p-value**	**q-value**
ABCC1	6.34 (6.03, 6.60)	6.68 (6.37, 7.41)	0.016	0.4
RAD21	8.14 (7.33, 8.59)	8.31 (7.42, 8.73)	0.7	>0.9
ATR	6.60 (6.28, 6.89)	6.43 (6.18, 6.64)	0.2	>0.9
ERBB2	8.19 (7.54, 8.71)	8.05 (7.58, 9.15)	>0.9	>0.9
SLX4	4.81 (4.38, 5.35)	5.06 (4.56, 5.25)	0.3	>0.9
ABCB1	2.77 (1.95, 3.78)	3.44 (2.18, 4.22)	0.4	>0.9
ABCC2	3.25 (2.18, 5.67)	2.34 (1.73, 5.84)	0.5	>0.9
ATM	6.28 (5.96, 6.65)	6.52 (6.13, 6.79)	0.3	>0.9
TOP1	6.92 (6.75, 7.24)	6.96 (6.72, 7.20)	0.8	>0.9
[1] Median (IQR)				

Table 4a: Somatic & transcriptomic landscape for acquired resistance to T-DXd

Somatic Profile				
Gene	**Baseline** N = 64	**AcqRes** N = 38	**p-value**	**q-value**
RAD21	3 (4.7%)	3 (7.9%)	0.7	>0.9
PALB2	2 (3.1%)	2 (5.3%)	0.6	>0.9
BRCA1	1 (1.6%)	1 (2.6%)	>0.9	>0.9
BRCA2	1 (1.6%)	1 (2.6%)	>0.9	>0.9
EMSY	1 (1.6%)	1 (2.6%)	>0.9	>0.9
ABCC3	0 (0%)	1 (2.6%)	0.4	>0.9
ATR	1 (1.6%)	0 (0%)	>0.9	>0.9
CHEK2	2 (3.1%)	1 (2.6%)	>0.9	>0.9
MSH2	1 (1.6%)	0 (0%)	>0.9	>0.9
Transcriptomic Profile				
Gene	**Baseline** N = 53[1]	**AcqRes** N = 26[1]	**p-value**	**q-value**
ABCB1	2.66 (1.96, 3.76)	3.35 (2.52, 4.41)	0.077	0.8
ABCC1	6.59 (6.28, 6.93)	6.39 (5.77, 6.78)	0.2	0.8
ABCC2	2.44 (1.92, 4.81)	3.38 (2.50, 4.79)	0.2	0.8
SLX4	4.56 (4.16, 5.12)	4.51 (4.20, 4.85)	0.4	>0.9
TOP1	7.04 (6.62, 7.30)	6.97 (6.55, 7.16)	0.4	>0.9
TACSTD2	7.49 (6.94, 8.37)	7.75 (6.24, 8.31)	0.8	>0.9
TOP2A	6.78 (6.09, 7.36)	6.92 (6.06, 7.45)	0.7	>0.9
RAD21	8.02 (7.71, 8.95)	8.21 (7.66, 8.76)	>0.9	>0.9
[1] Median (IQR)				

Table 4b: Somatic & transcriptomic landscape for acquired resistance to SG

Somatic Profile				
Gene	**Baseline** N = 42	**AcqRes** N = 15	**p-value**	**q-value**
ERBB2	29 (69%)	6 (40%)	**0.047**	>0.9
ABCC3	4 (9.5%)	0 (0%)	0.6	>0.9
Transcriptomic Profile				
Gene	**Baseline** N = 34[1]	**AcqRes** N = 10[1]	**p-value**	**q-value**
ERBB2	10.91 (9.29, 11.50)	8.44 (7.68, 9.81)	**0.024**	0.3
ABCC1	6.34 (5.94, 6.73)	6.83 (6.17, 6.92)	0.054	0.3
ABCB1	3.34 (2.32, 4.01)	2.71 (1.63, 3.25)	0.075	0.4
ABCC2	3.19 (2.34, 5.08)	3.18 (1.95, 3.66)	0.2	0.6
[1] Median (IQR)				

Table 4c: Somatic & transcriptomic landscape for acquired resistance to T-DM1

Somatic Profile				
Gene	**PrRes** **Pre-or-Post-T-DXd$_{tx}$** **Duration 0-3 months** N = 26	**Baseline** **Pre-T-DXd$_{tx}$** **Duration: > 3 months** N = 67	**p-value**	**q-value**
ERBB2	4 (15%)	18 (27%)	0.2	>0.9
ABCC3	0 (0%)	4 (6.0%)	0.6	>0.9
ATM	1 (3.8%)	0 (0%)	0.3	>0.9
TOP1	1 (3.8%)	0 (0%)	0.3	>0.9
BRCA1	0 (0%)	1 (1.5%)	>0.9	>0.9
Transcriptomic Profile				
Gene	**PrRes** N = 22[1]	**Baseline** N = 57[1]	**p-value**	**q-value**
ERBB2	7.81 (7.39, 8.14)	8.19 (7.54, 8.71)	0.062	0.6
ABCB1	3.18 (2.30, 4.82)	2.77 (1.95, 3.78)	0.074	0.6
ATM	5.97 (5.82, 6.45)	6.28 (5.96, 6.65)	0.12	0.7
ABCC1	6.38 (6.23, 6.74)	6.34 (6.03, 6.60)	0.3	0.9
ABCC2	2.64 (2.13, 5.35)	3.25 (2.18, 5.67)	0.6	>0.9
TOP1	7.02 (6.66, 7.24)	6.92 (6.75, 7.24)	0.8	>0.9
SLX4	4.89 (4.47, 5.26)	4.81 (4.38, 5.35)	>0.9	>0.9
[1] Median (IQR)				

Table 5a: Somatic & transcriptomic landscape for primary resistance to T-DXd

Somatic Profile				
Gene	**PrRes** N = 55	**Baseline** N = 64	**p-value**	**q-value**
EMSY	2 (3.6%)	1 (1.6%)	0.6	>0.9
CHEK2	1 (1.8%)	2 (3.1%)	>0.9	>0.9
PALB2	0 (0%)	2 (3.1%)	0.5	>0.9
BRCA1	1 (1.8%)	1 (1.6%)	>0.9	>0.9
BRCA2	1 (1.8%)	1 (1.6%)	>0.9	>0.9
MSH2	1 (1.8%)	1 (1.6%)	>0.9	>0.9
Transcriptomic Profile				
Gene	**PrRes** N = 51[1]	**Baseline** N = 53[1]	**p-value**	**q-value**
ABCC1	6.38 (5.93, 6.86)	6.59 (6.28, 6.93)	0.2	0.6
TACSTD2	7.21 (6.15, 7.90)	7.49 (6.94, 8.37)	0.2	0.6
SLX4	4.59 (4.17, 4.89)	4.56 (4.16, 5.12)	0.5	0.8
ABCB1	2.84 (1.88, 4.01)	2.66 (1.96, 3.76)	0.6	0.8
TOP1	7.03 (6.78, 7.28)	7.04 (6.62, 7.30)	0.7	0.8
ABCC2	2.96 (1.88, 4.94)	2.44 (1.92, 4.81)	0.7	0.8
[1] Median (IQR)				

Table 5b: Somatic & transcriptomic landscape for primary resistance to SG

Somatic Profile				
Gene	**PrRes** N = 27	**Baseline** N = 42	**p-value**	**q-value**
ERBB2	13 (48%)	29 (69%)	0.083	>0.9
ABCC3	0 (0%)	4 (9.5%)	0.15	>0.9
Transcriptomic Profile				
Gene	**PrRes** N = 24[1]	**Baseline** N = 34[1]	**p-value**	**q-value**
ERBB2	8.76 (7.98, 10.95)	10.91 (9.29, 11.50)	**0.02**	0.4
ABCC1	6.29 (6.17, 6.85)	6.34 (5.94, 6.73)	0.2	0.6
ABCC2	2.79 (1.90, 4.74)	3.19 (2.34, 5.08)	0.4	0.8
ABCB1	2.90 (2.11, 4.10)	3.34 (2.32, 4.01)	0.8	>0.9
[1] Median (IQR)				

Table 5c: Somatic & transcriptomic landscape for primary resistance to T-DM1

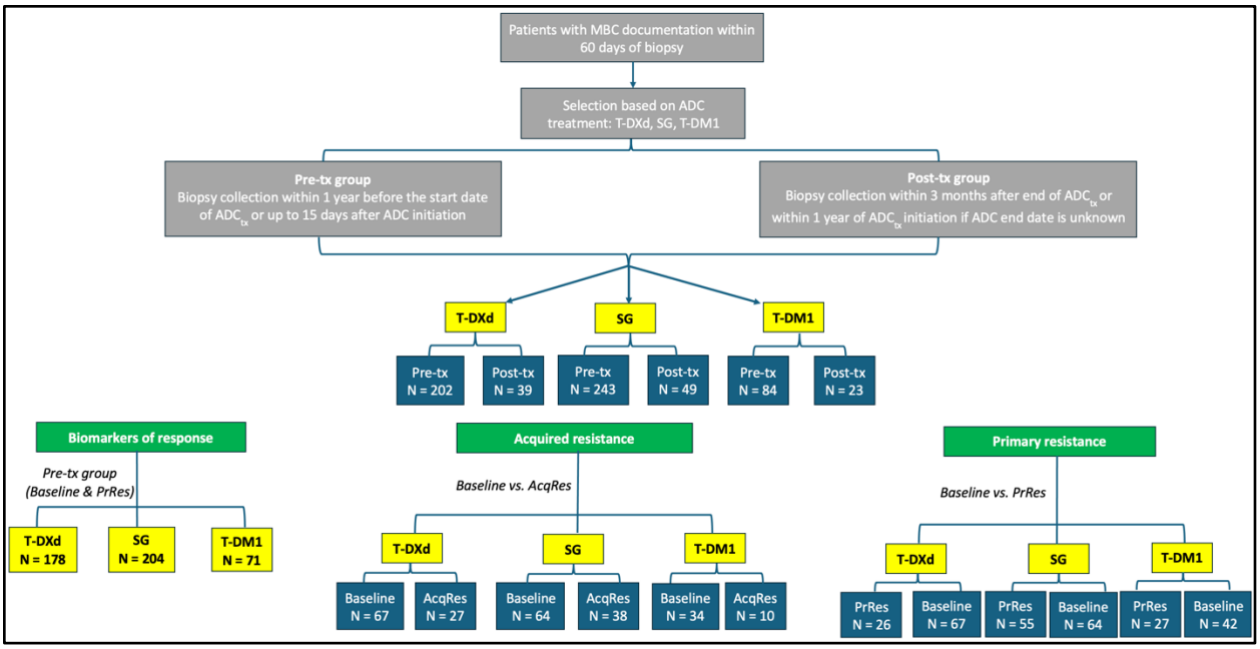

Figure 1: Study Design. **Baseline profile:** pre-treatment samples from patients who did not exhibit primary resistance (treated with ADC for > 3 months). **Primary resistance (PrRes):** pre- and post-treatment samples from patients treated with ADC for 0-3 months. **Acquired resistance (AcqRes):** post-treatment samples from patients treated with ADC for > 3 months.

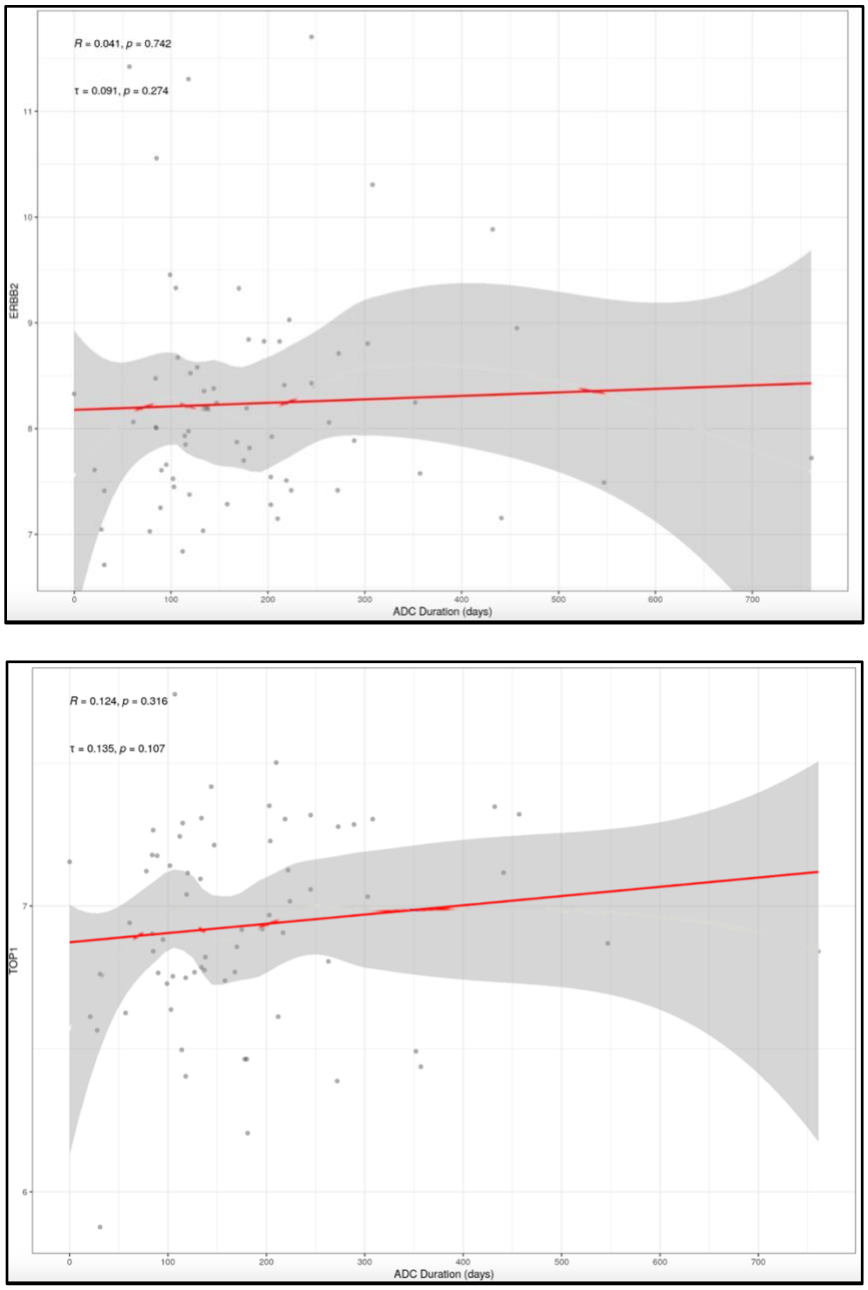

Figure 2a: Scatterplot of pre-treatment transcriptomic profile vs. duration of T-DXd treatment

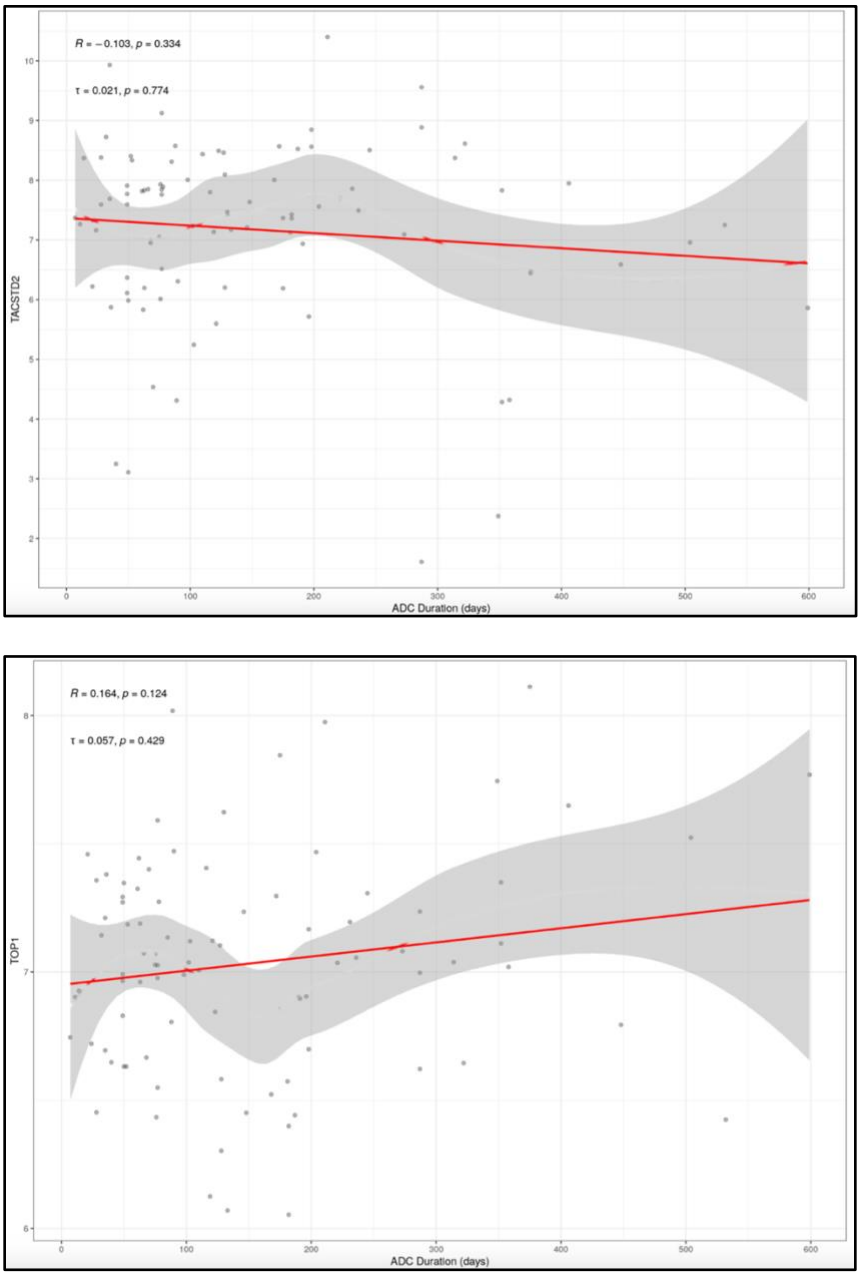

Figure 2b: Scatterplot of pre-treatment transcriptomic profile vs. duration of SG treatment

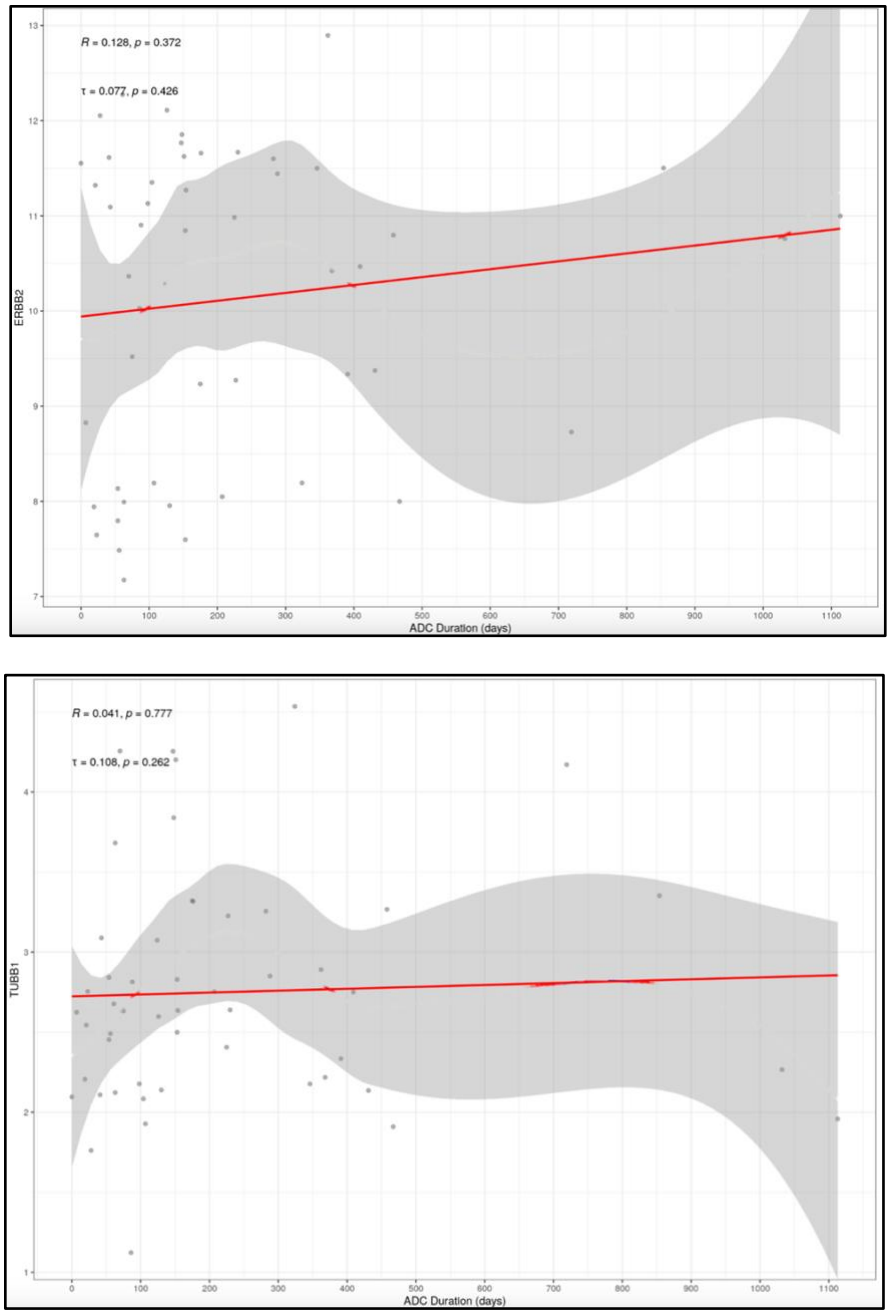

Figure 2c: Scatterplot of pre-treatment transcriptomic profile vs. duration of T-DM1 treatment

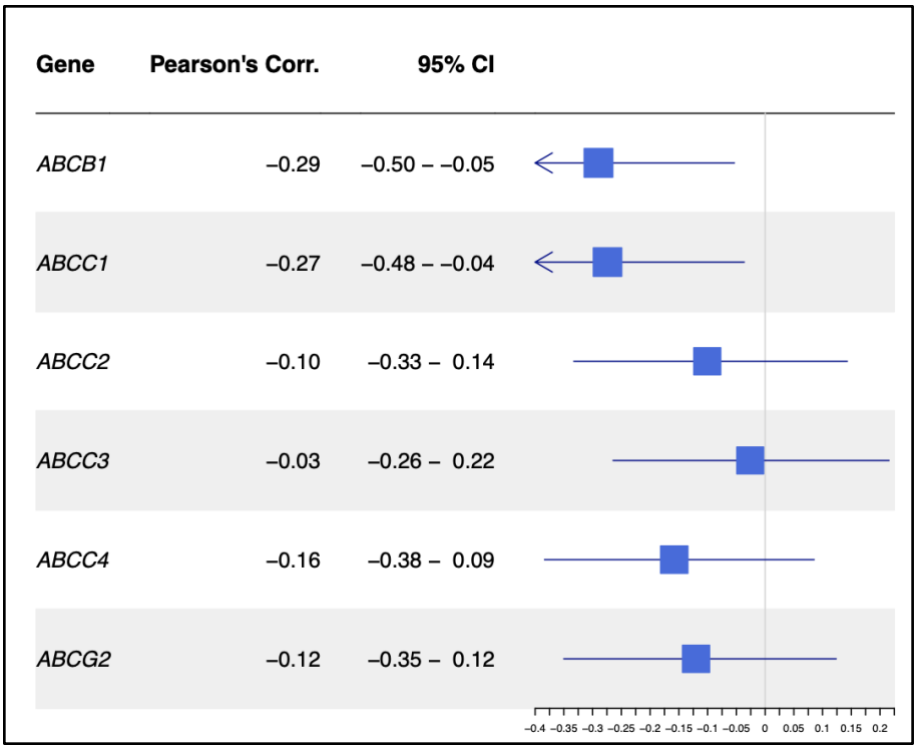

Figure 3a: Correlation Between Efflux Pump Gene Expression and T-DXd DoT

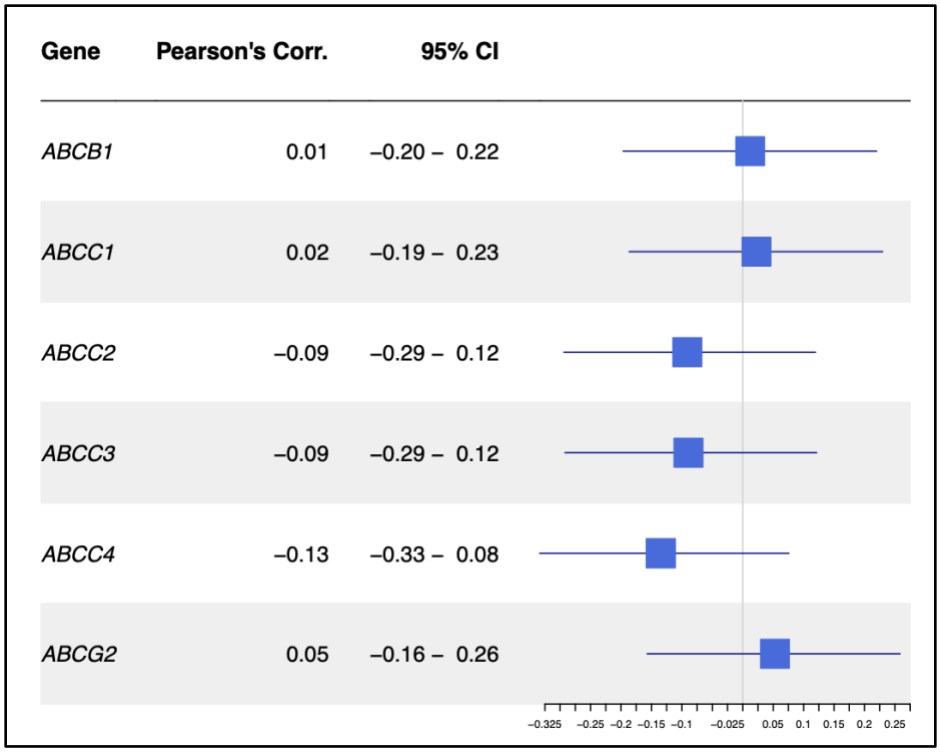

Figure 3b: Correlation Between Efflux Pump Gene Expression and SG DoT

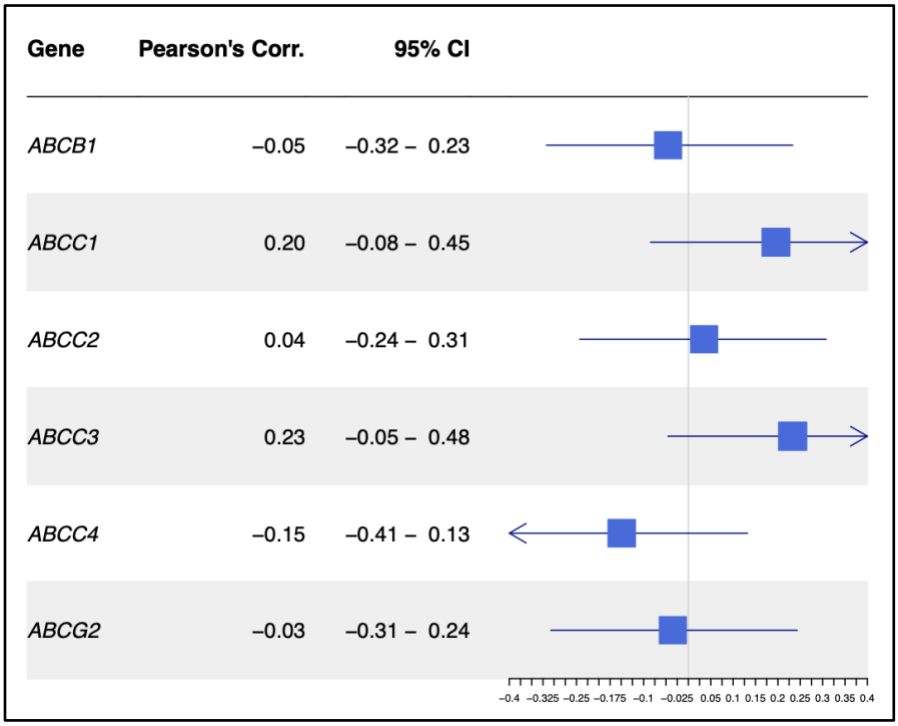

Figure 3c: Correlation Between Efflux Pump Gene Expression and T-DM1 DoT

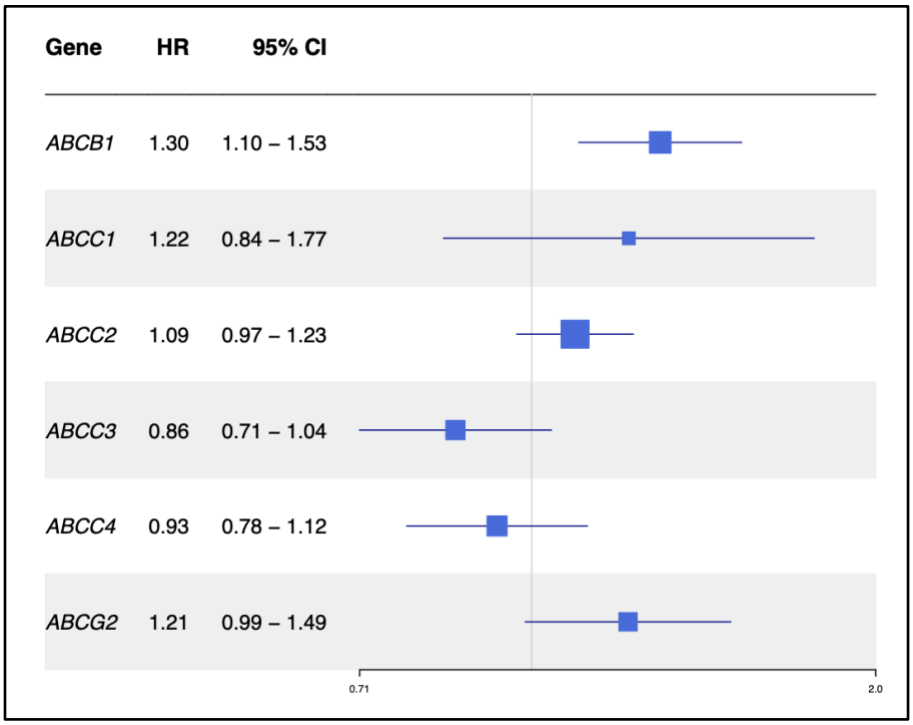

Figure 4a: Correlation Between Efflux Pump Gene Expression and OS Following T-DXd Treatment

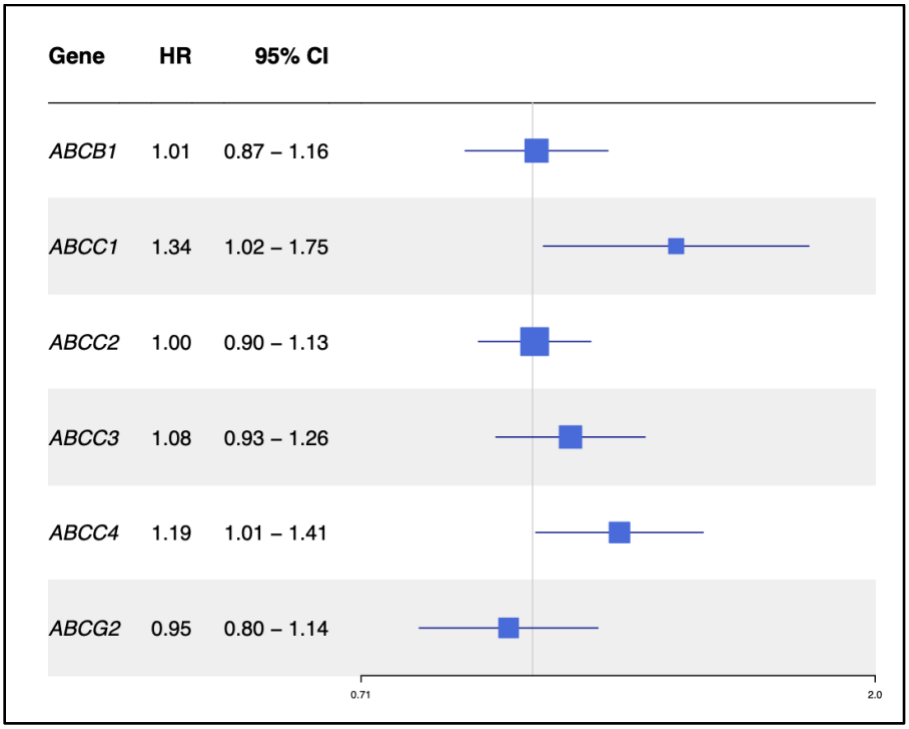

Figure 4b: Correlation Between Efflux Pump Gene Expression and OS Following SG Treatment

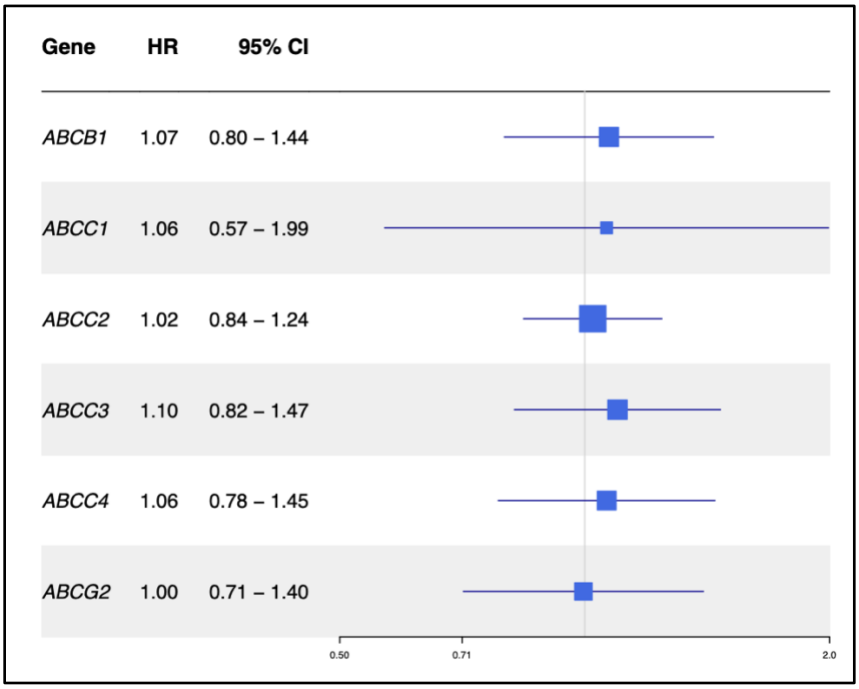

Figure 4c: Correlation Between Efflux Pump Gene Expression and OS Following T-DM1 Treatment

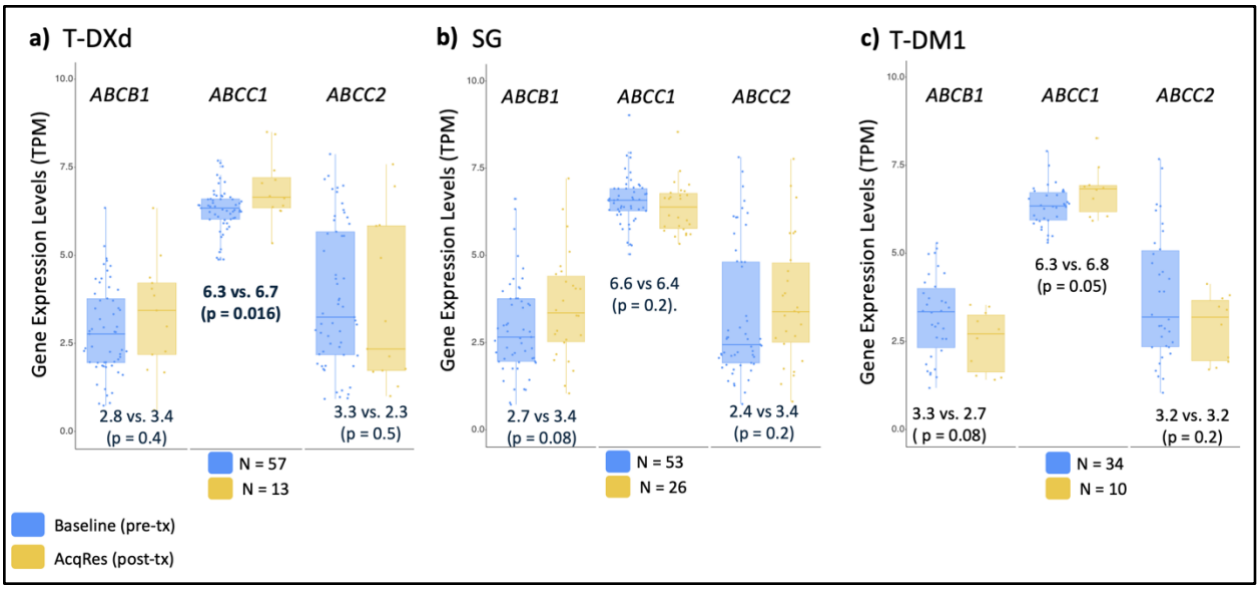

Figure 5: Expression of efflux pump genes in the baseline vs. acquired resistance cohorts. There was a trend toward higher expression across efflux pump genes for patients with acquired resistance to SG in *ABCB1* and *ABCC2*. Among patients treated with T-DXd, efflux pump gene expression in the AcqRes cohort was higher than the pre-tx baseline cohort for *ABCC1* and *ABCB1*. T-DM1 was associated with less noticeable changes in efflux genes.

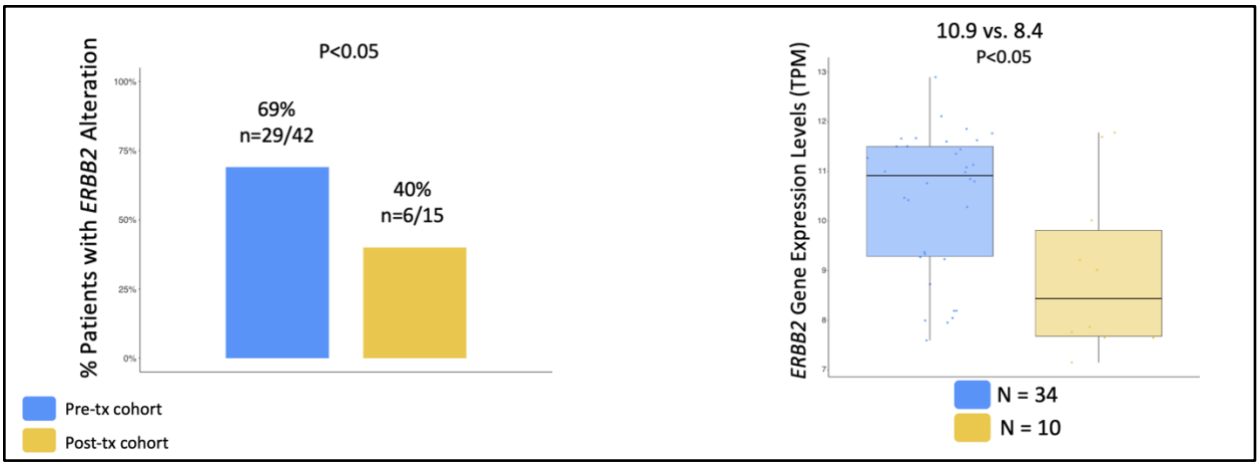

Figure 6: ERBB2 status in acquired resistance to T-DM1. Patients with acquired resistance to T-DM1 exhibited lower frequency of ERBB2 alterations and lower levels of ERBB2 expression compared to pre-treatment baseline samples

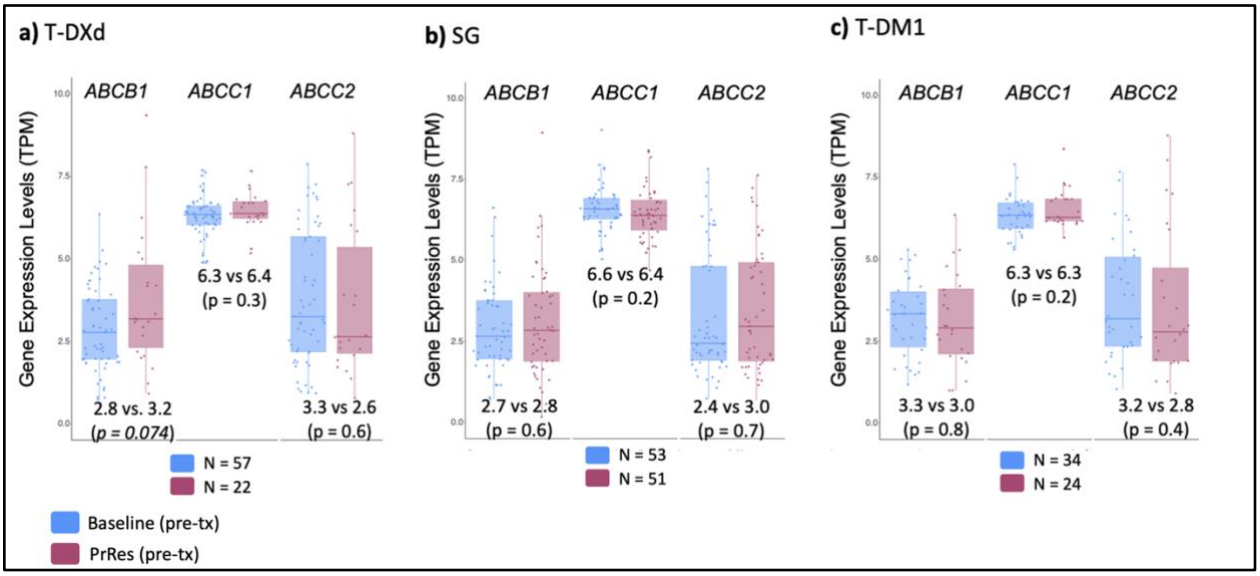

Figure 7: Expression of efflux pump genes in the baseline vs. primary resistance cohorts. A trend of higher efflux pump gene expression was associated with primary resistance to T-DXd in ABCB1.

APPENDICES

Extended Data Tables and Figures:

	T-DXd			SG			T-DM1		
Gene	***r*** **(DoT)**	**HR (95% CI)**	**p-value**	***r*** **(DoT)**	**HR (95% CI)**	**p-value**	***r*** **(DoT)**	**HR (95% CI)**	***p***
Internalization and Trafficking									
CLTC	0.237	0.883 (0.604 - 1.289)	0.52	-0.139	1.342 (0.985 - 1.828)	0.06	0.011	0.612 (0.322 - 1.162)	0.13
DNM2	0.066	**0.449 (0.238 - 0.849)**	**0.014**	-0.064	0.967 (0.583 - 1.604)	0.9	-0.041	2.884 (0.846 - 9.826)	0.09
SH3GL1	0.053	1.579 (0.968 - 2.576)	0.07	-0.089	0.717 (0.444 - 1.158)	0.17	-0.125	1.536 (0.534 - 4.423)	0.43
CAV1	-0.156	1.009 (0.820 - 1.241)	0.94	0.024	0.997 (0.877 - 1.134)	0.97	0.087	1.179 (0.827 - 1.682)	0.36
RABGAP1	0.035	0.938 (0.572 - 1.539)	0.80	-0.019	0.797 (0.544 - 1.167)	0.24	-0.107	0.859 (0.455 - 1.622)	0.64
HECTD1	-0.051	1.368 (0.798 - 2.345)	0.26	0.211	0.976 (0.635 - 1.501)	0.91	-0.021	1.720 (0.948 - 3.120)	0.07
DNA Damage Repair Proteins									
MSH2	-0.063	1.439 (0.964 - 2.149)	0.08	0.145	1.150 (0.873 - 1.515)	0.32			
MSH6	-0.024	1.424 (0.912 - 2.224)	0.12	0.085	1.292 (0.871 - 1.917)	0.20			
MLH1	-0.147	1.095 (0.674 - 1.780)	0.71	0.155	0.701 (0.450 - 1.090)	0.12			
PMS2	-0.135	1.430 (0.803 - 2.545)	0.22	0.205	0.799 (0.557 - 1.146)	0.22			
ATR	-0.065	1.217 (0.726 - 2.039)	0.46	0.139	0.991 (0.736 - 1.333)	0.95			
RAD52	-0.049	1.417 (0.906 - 2.216)	0.13	0.271	0.913 (0.707 - 1.178)	0.48			
PALB2	0.012	1.012 (0.622 - 1.646)	0.96	-0.004	1.254 (0.870 - 1.808)	0.23			
BRCA1	-0.043	0.979 (0.738 - 1.301)	0.89	-0.185	1.193 (0.970 - 1.467)	0.1			
BRCA2	0.078	0.884 (0.660 - 1.182)	0.41	0.155	1.113 (0.891 - 1.392)	0.35			
CHEK2	0.045	1.227 (0.841 - 1.790)	0.29	0.073	1.261 (0.950 - 1.673)	0.11			
TP53	0.049	1.116 (0.806 - 1.547)	0.51	0.188	0.817 (0.658 - 1.015)	0.07			
ATM	-0.172	0.930 (0.628 - 1.379)	0.72	0.153	0.821 (0.611 - 1.102)	0.19			
RECQL4	0.355	1.062 (0.843 - 1.336)	0.61	0.035	1.177 (0.974 - 1.423)	0.09			
BRIP1	-0.004	1.113 (0.863 - 1.435)	0.41	0.114	0.942 (0.771 - 1.151)	0.56			
MUTYH	-0.072	0.907 (0.590 - 1.394)	0.66	0.178	1.110 (0.764 - 1.613)	0.58			
ERCC3	-0.027	2.029 (0.988 - 4.170)	0.05	0.171	0.648 (0.396 - 1.058)	0.08			
RAD50	-0.043	0.999 (0.605 - 1.652)	0.998	0.012	0.746 - 1.611	0.64			
CUL4A	0.170	0.793 (0.472 - 1.331)	0.38	0.076	0.926 (0.656 - 1.309)	0.67			
Lysosomal Function									
SLC46A3	-0.048	0.924	0.55	-0.106	1.198	0.1	0.014	1.192	0.41

		(0.713 - 1.198)			(0.969 - 1.482)			(0.788 - 1.801)	
RAB5B	0.064	0.612 (0.293 - 1.280)	0.19	0.030	0.656 (0.371 - 1.162)	0.15	0.025	0.391 (0.100 - 1.530)	0.18
ATG9A	-0.047	**2.044 (1.081 - 3.866)**	**0.03**	-0.073	1.297 (0.822 - 2.045)	0.26	-0.089	0.606 (0.207 - 1.776)	0.36
RAB6A	-0.037	1.204 (0.871 - 1.663)	0.26	0.001			-0.101	1.723 (0.775 - 3.833)	0.18
RAB6B	-0.037	0.906 (0.732 - 1.121)	0.36	0.163	1.116 (0.930 - 1.338)	0.238	-0.252	**1.483 (1.116 - 1.971)**	**0.007**
RAB6C	0.058	0.934 (0.781 - 1.117)	0.46	0.055	0.953 (0.791 - 1.150)	0.62	0.096	0.771 (0.577 - 1.029)	0.08
RAB6D	0.181	0.905 (0.756 - 1.084)	0.28	-0.036	0.945 (0.794 - 1.125)	0.53	0.180	0.814 (0.573 - 1.156)	0.25
PAK4	0.049	0.877 (0.654 - 1.178)	0.38	0.088	0.986 (0.765 - 1.272)	0.91	0.108		
LAMP2	-0.153	1.085 (0.691 - 1.706)	0.72	-0.193	**1.354 (1.018 - 1.802)**	**0.04**	-0.340	0.637 (0.289 - 1.406)	0.27
LYSET	0.055	0.975 (0.618 - 1.539)	0.91	0.008	1.062 (0.748 - 1.508)	0.74	0.079	0.989 (0.458 - 2.135)	0.98
CTSB	-0.038	0.928 (0.672 - 1.282)	0.65	**-0.215**	**1.457 (1.097 - 1.936)**	**0.009**	0.150	1.030 (0.620 - 1.710)	0.91
Signal Transduction									
ROR1	-0.141	1.120 (0.909 - 1.381)	0.29	-0.057	1.087 (0.905 - 1.305)	0.37	-0.158		
YES1	-0.115	**1.350 (1.007 - 1.810)**	**0.045**	0.070	0.997 (0.776 - 1.280)	0.98	-0.141	0.789 (0.464 - 1.342)	0.38
PIK/AKT Pathway									
PIK3CA	-0.098	1.131 (0.703 - 1.819)	0.61	0.175	0.753 (0.519 - 1.094)	0.14	-0.112	1.766 (0.661 - 4.714)	0.26
PIK3R1	-0.266	0.873 (0.636 - 1.197)	0.40	0.028	0.862 (0.669 - 1.110)	0.25	-0.052	0.707 (0.415 - 1.204)	0.20
PTEN	-0.078	0.802 (0.522 - 1.234)	0.32	0.118			-0.232	0.806 (0.412 - 1.578)	0.53
MTOR	0.003	0.615 (0.318 - 1.189)	0.15	0.233	1.119 (0.697 - 1.796)	0.64	0.148	0.660 (0.215 - 2.027)	0.47
AKT1	0.192	0.729 (0.464 - 1.146)	0.17	-0.206	1.016 (0.767 - 1.347)	0.91	0.363	0.817 (0.479 - 1.394)	0.46
AKT2	0.009	1.120 (0.711 - 1.764)	0.63	0.213	0.735 (0.493 - 1.096)	0.13	-0.137	0.838 (0.360 - 1.950)	0.68
AKT3	-0.179	1.031 (0.830 - 1.281)	0.78	-0.058	0.988 (0.837 - 1.167)	0.89	0.054	0.997 (0.693 - 1.434)	0.99
TSC1	-0.215	1.305 (0.766 - 2.222)	0.33	-0.044	0.715 (0.483 - 1.058)	0.1	0.211		
RAS/MAPK Pathway									
KRAS	0.179	1.028 (0.699 - 1.513)	0.89	0.163	0.927 (0.677 - 1.268)	0.63	-0.045	1.071 (0.435 - 2.637)	0.88
HRAS	0.161	0.935 (0.640 - 1.365)	0.73	0.033	1.096 (0.786 - 1.528)	0.59	0.146	1.018 (0.520 - 1.992)	0.96
BRAF	0.020	0.910 (0.589 - 1.404)	0.67	0.163			0.078	0.813 (0.372 - 1.776)	0.60
MAP2K1	0.122	0.750 (0.406 - 1.388)	0.36	-0.059	0.908 (0.576 - 1.432)	0.68	0.022	1.051 (0.327 - 3.376)	0.93
MAP2K4	-0.134	1.379 (0.984 - 1.932)	0.06	0.153	**0.566 (0.378 - 0.849)**	**0.006**	-0.038	0.846 (0.391 - 1.831)	0.67
MAP3K1	0.035	0.806 (0.573 - 1.133)	0.22	0.045	0.901 (0.673 - 1.206)	0.48	0.058	**0.410 (0.198 - 0.851)**	**0.02**
PPM1D	0.103	1.007 (0.724 - 1.403)	0.97	0.101	0.689 (0.469 - 1.008)	0.056	-0.115	0.834 (0.484 - 1.438)	0.51

Extended Data Table 1: Biomarkers of response, correlation with duration of treatment (DoT) and overall survival (OS). ***r*:** Pearson's correlation coefficient

Somatic Profile				
Gene	**Baseline Pre-T-DXd$_{tx}$** N = 67	**AcqRes Post-T-DXd$_{tx}$** N = 27	**p-value**	**q-value**
TP53	38 (57%)	14 (52%)	0.7	>0.9
PIK3CA	30 (45%)	10 (37%)	0.5	>0.9
PTEN	10 (15%)	6 (22%)	0.4	>0.9
PPM1D	5 (7.5%)	3 (11%)	0.7	>0.9
RECQL4	3 (4.5%)	2 (7.4%)	0.6	>0.9
MAP2K4	5 (7.5%)	0 (0%)	0.3	>0.9
MAP3K1	3 (4.5%)	0 (0%)	0.6	>0.9
AKT2	2 (3.0%)	1 (3.7%)	>0.9	>0.9
PIK3R1	0 (0%)	1 (3.7%)	0.3	>0.9
BRIP1	2 (3.0%)	0 (0%)	>0.9	>0.9
ERCC3	2 (3.0%)	0 (0%)	>0.9	>0.9
KRAS	2 (3.0%)	0 (0%)	>0.9	>0.9
AKT1	1 (1.5%)	0 (0%)	>0.9	>0.9
DNM2	1 (1.5%)	0 (0%)	>0.9	>0.9
MAP2K1	1 (1.5%)	0 (0%)	>0.9	>0.9
MAP3K7	1 (1.5%)	0 (0%)	>0.9	>0.9
Transcriptomic Profile				
Gene	**Baseline** N = 57[1]	**AcqRes** N = 13[1]	**p-value**	**q-value**
ATR	6.60 (6.28, 6.89)	6.43 (6.18, 6.64)	0.2	>0.9
ATM	6.28 (5.96, 6.65)	6.52 (6.13, 6.79)	0.3	>0.9
ROR1	2.75 (1.64, 3.62)	1.96 (1.49, 2.50)	0.3	>0.9
SLX4	4.81 (4.38, 5.35)	5.06 (4.56, 5.25)	0.3	>0.9
RAD52	5.12 (4.85, 5.49)	5.21 (5.04, 5.50)	0.6	>0.9
PIK3CA	4.33 (4.10, 4.65)	4.36 (4.22, 4.51)	0.8	>0.9
PTEN	5.49 (5.07, 5.81)	5.62 (5.35, 5.66)	0.9	>0.9
YES1	5.92 (5.47, 6.34)	6.07 (5.34, 6.44)	0.9	>0.9
[1] Median (IQR)				

Extended Data Table 2a: Somatic & transcriptomic landscape of acquired resistance to T-DXd

Somatic Profile				
Gene	**Baseline** N = 64	**AcqRes** N = 38	**p-value**	**q-value**
TP53	52 (81%)	31 (82%)	>0.9	>0.9
PIK3CA	8 (13%)	10 (26%)	0.08	>0.9
PTEN	8 (13%)	5 (13%)	>0.9	>0.9
PIK3R1	2 (3.1%)	3 (7.9%)	0.4	>0.9
PPM1D	0 (0%)	3 (7.9%)	0.05	>0.9
AKT1	1 (1.6%)	2 (5.3%)	0.6	>0.9
DNM2	0 (0%)	2 (5.3%)	0.14	>0.9
MAP3K1	3 (4.7%)	2 (5.3%)	>0.9	>0.9
AKT2	3 (4.7%)	0 (0%)	0.3	>0.9
RECQL4	3 (4.7%)	1 (2.6%)	>0.9	>0.9
ERCC3	2 (3.1%)	0 (0%)	0.5	>0.9
KRAS	2 (3.1%)	1 (2.6%)	>0.9	>0.9
MAP2K4	2 (3.1%)	0 (0%)	0.5	>0.9
BRIP1	0 (0%)	1 (2.6%)	0.4	>0.9
MUTYH	0 (0%)	1 (2.6%)	0.4	>0.9
TSC1	1 (1.6%)	1 (2.6%)	>0.9	>0.9
BRAF	1 (1.6%)	0 (0%)	>0.9	>0.9
CUL4A	1 (1.6%)	0 (0%)	>0.9	>0.9
HRAS	1 (1.6%)	0 (0%)	>0.9	>0.9
RAD50	1 (1.6%)	0 (0%)	>0.9	>0.9
Transcriptomic Profile				
Gene	**Baseline** N = 53[1]	**AcqRes** N = 26[1]	**p-value**	**q-value**
PIK3CA	4.41 (4.07, 4.65)	4.49 (4.33, 4.92)	0.2	0.8
ATM	6.34 (6.00, 6.91)	6.30 (6.04, 6.58)	0.5	>0.9
YES1	6.35 (5.85, 6.92)	6.33 (6.08, 6.98)	0.6	>0.9
RAD52	5.21 (4.68, 5.60)	5.25 (4.79, 5.84)	0.6	>0.9
ATR	6.98 (6.43, 7.20)	6.75 (6.31, 7.17)	0.6	>0.9
ROR1	3.04 (2.17, 3.96)	3.26 (2.34, 3.89)	0.7	>0.9
PTEN	5.41 (5.04, 5.71)	5.48 (4.97, 5.62)	0.8	>0.9
[1] Median (IQR)				

Extended Data Table 2b: Somatic & transcriptomic landscape of acquired resistance to SG

Somatic Profile				
Gene	**Baseline** N = 42	**AcqRes** N = 15	**p-value**	**q-value**
TP53	26 (62%)	10 (67%)	0.7	>0.9
PIK3CA	14 (33%)	5 (33%)	>0.9	>0.9
PTEN	2 (4.8%)	2 (13%)	0.3	>0.9
PPM1D	5 (12%)	0 (0%)	0.3	>0.9
EMSY	1 (2.4%)	1 (6.7%)	0.5	>0.9
MAP2K4	2 (4.8%)	1 (6.7%)	>0.9	>0.9
RECQL4	0 (0%)	1 (6.7%)	0.3	>0.9
KRAS	2 (4.8%)	0 (0%)	>0.9	>0.9
MAP3K1	2 (4.8%)	0 (0%)	>0.9	>0.9
AKT3	1 (2.4%)	0 (0%)	>0.9	>0.9
ATM	1 (2.4%)	0 (0%)	>0.9	>0.9
BRCA2	1 (2.4%)	0 (0%)	>0.9	>0.9
MSH2	1 (2.4%)	0 (0%)	>0.9	>0.9
PALB2	1 (2.4%)	0 (0%)	>0.9	>0.9
PIK3R1	1 (2.4%)	0 (0%)	>0.9	>0.9
Transcriptomic Profile				
Gene	**Baseline** N = 34[1]	**AcqRes** N = 10[1]	**p-value**	**q-value**
ROR1	2.13 (1.67, 3.26)	3.22 (3.03, 3.88)	**0.02**	0.3
ATR	6.56 (6.48, 6.86)	6.63 (6.31, 6.82)	0.6	>0.9
RAD52	5.06 (4.67, 5.32)	5.10 (4.90, 5.50)	0.6	>0.9
PIK3CA	4.31 (4.07, 4.49)	4.37 (4.21, 4.51)	0.6	>0.9
SLX4	4.86 (4.56, 5.30)	4.91 (4.75, 5.31)	0.7	>0.9
ATM	6.43 (5.95, 6.61)	6.40 (6.17, 6.53)	0.8	>0.9
[1] Median (IQR)				

Extended Data Table 2c: Somatic & transcriptomic landscape of acquired resistance to T-DM1

Somatic Profile				
Gene	**PrRes** **Pre-T-DXd$_{tx}$ Duration 0-3 months** N = 26	**Baseline** **Bx Pre-T-DXd$_{tx}$ Duration: > 3 months** N = 67	**p-value**	**q-value**
TP53	11 (42%)	38 (57%)	0.2	>0.9
PIK3CA	7 (27%)	30 (45%)	0.11	>0.9
PTEN	3 (12%)	10 (15%)	>0.9	>0.9
MAP2K4	2 (7.7%)	5 (7.5%)	>0.9	>0.9
MAP3K1	2 (7.7%)	3 (4.5%)	0.6	>0.9
PIK3R1	2 (7.7%)	0 (0%)	0.076	>0.9

PPM1D	1 (3.8%)	5 (7.5%)	>0.9	>0.9
RECQL4	1 (3.8%)	3 (4.5%)	>0.9	>0.9
AKT2	1 (3.8%)	2 (3.0%)	>0.9	>0.9
BRAF	1 (3.8%)	0 (0%)	0.3	>0.9
EMSY	1 (3.8%)	2 (3.0%)	>0.9	>0.9
MSH3	1 (3.8%)	0 (0%)	0.3	>0.9
MSH6	1 (3.8%)	0 (0%)	0.3	>0.9
ATR	0 (0%)	2 (3.0%)	>0.9	>0.9
BRIP1	0 (0%)	2 (3.0%)	>0.9	>0.9
ERCC3	0 (0%)	2 (3.0%)	>0.9	>0.9
KRAS	0 (0%)	2 (3.0%)	>0.9	>0.9
AKT1	0 (0%)	1 (1.5%)	>0.9	>0.9
CHEK2	0 (0%)	1 (1.5%)	>0.9	>0.9
DNM2	0 (0%)	1 (1.5%)	>0.9	>0.9
MAP2K1	0 (0%)	1 (1.5%)	>0.9	>0.9
MAP3K7	0 (0%)	1 (1.5%)	>0.9	>0.9
Transcriptomic Profile				
Gene	**PrRes** N = 22[1]	**Baseline** N = 57[1]	**p-value**	**q-value**
RAD52	5.09 (4.62, 5.33)	5.12 (4.85, 5.49)	0.5	>0.9
ROR1	2.30 (1.50, 3.43)	2.75 (1.64, 3.62)	0.5	>0.9
PIK3CA	4.41 (4.08, 4.68)	4.33 (4.10, 4.65)	0.8	>0.9
YES1	6.01 (5.40, 6.58)	5.92 (5.47, 6.34)	0.9	>0.9
PTEN	5.50 (5.19, 5.63)	5.49 (5.07, 5.81)	>0.9	>0.9
[1] Median (IQR)				

Extended Data Table 3a: Somatic & transcriptomic landscape of primary resistance to T-DXd

Somatic Profile				
Gene	**PrRes** N = 55	**Baseline** N = 64	**p-value**	**q-value**
TP53	46 (84%)	52 (81%)	0.7	>0.9
PIK3CA	14 (25%)	8 (13%)	0.07	>0.9
PTEN	10 (18%)	8 (13%)	0.4	>0.9
AKT1	3 (5.5%)	1 (1.6%)	0.3	>0.9
MAP2K4	3 (5.5%)	2 (3.1%)	0.7	>0.9
AKT2	0 (0%)	3 (4.7%)	0.2	>0.9
MAP3K1	2 (3.6%)	3 (4.7%)	>0.9	>0.9
ERCC3	0 (0%)	2 (3.1%)	0.5	>0.9
KRAS	1 (1.8%)	2 (3.1%)	>0.9	>0.9
PIK3R1	1 (1.8%)	2 (3.1%)	>0.9	>0.9
ATR	1 (1.8%)	1 (1.6%)	>0.9	>0.9
BRAF	1 (1.8%)	1 (1.6%)	>0.9	>0.9
BRIP1	1 (1.8%)	0 (0%)	0.5	>0.9
MTOR	1 (1.8%)	0 (0%)	0.5	>0.9
CUL4A	0 (0%)	1 (1.6%)	>0.9	>0.9
HRAS	0 (0%)	1 (1.6%)	>0.9	>0.9
RAD50	0 (0%)	1 (1.6%)	>0.9	>0.9
TSC1	0 (0%)	1 (1.6%)	>0.9	>0.9
Transcriptomic Profile				
Gene	**PrRes** N = 51[1]	**Baseline** N = 53[1]	**p-value**	**q-value**
RAD52	4.86 (4.64, 5.25)	5.21 (4.68, 5.60)	0.05	0.3
YES1	6.19 (5.62, 6.66)	6.35 (5.85, 6.92)	0.2	0.6
ATM	6.24 (5.89, 6.68)	6.34 (6.00, 6.91)	0.3	0.6
ATR	6.72 (6.42, 7.02)	6.98 (6.43, 7.20)	0.3	0.6
PTEN	5.29 (4.82, 5.79)	5.41 (5.04, 5.71)	0.5	0.8
ROR1	2.77 (2.03, 3.84)	3.04 (2.17, 3.96)	0.6	0.8
PIK3CA	4.25 (3.94, 4.68)	4.41 (4.07, 4.65)	0.7	0.8

[1] Median (IQR)

Extended Data Table 3b: Somatic & transcriptomic landscape for primary resistance to SG

Somatic Profile				
Gene	**PrRes** N = 27	**Baseline** N = 42	**p-value**	**q-value**
TP53	18 (67%)	26 (62%)	0.7	>0.9
PIK3CA	14 (52%)	14 (33%)	0.13	>0.9
MAP3K1	4 (15%)	2 (4.8%)	0.2	>0.9
PPM1D	1 (3.7%)	5 (12%)	0.4	>0.9
BRCA2	3 (11%)	1 (2.4%)	0.3	>0.9
BRAF	2 (7.4%)	0 (0%)	0.15	>0.9
PTEN	2 (7.4%)	2 (4.8%)	0.6	>0.9
RECQL4	2 (7.4%)	0 (0%)	0.15	>0.9
KRAS	0 (0%)	2 (4.8%)	0.5	>0.9
MAP2K4	1 (3.7%)	2 (4.8%)	>0.9	>0.9
ERCC3	1 (3.7%)	0 (0%)	0.4	>0.9
MAP3K7	1 (3.7%)	0 (0%)	0.4	>0.9
PIK3R1	1 (3.7%)	1 (2.4%)	>0.9	>0.9
AKT3	0 (0%)	1 (2.4%)	>0.9	>0.9
ATM	0 (0%)	1 (2.4%)	>0.9	>0.9
EMSY	0 (0%)	1 (2.4%)	>0.9	>0.9
MSH2	0 (0%)	1 (2.4%)	>0.9	>0.9
PALB2	0 (0%)	1 (2.4%)	>0.9	>0.9
Transcriptomic Profile				
Gene	**PrRes** N = 24[1]	**Baseline** N = 34[1]	**p-value**	**q-value**
ATM	6.16 (5.85, 6.37)	6.43 (5.95, 6.61)	0.12	0.6
ROR1	2.55 (2.22, 3.31)	2.13 (1.67, 3.26)	0.2	0.6
SLX4	4.83 (4.39, 5.04)	4.86 (4.56, 5.30)	0.2	0.7
PTEN	5.31 (5.12, 5.92)	5.66 (5.23, 5.93)	0.2	0.7
ATR	6.77 (6.09, 7.09)	6.56 (6.48, 6.86)	0.5	0.8
RAD52	4.92 (4.63, 5.26)	5.06 (4.67, 5.32)	0.6	0.8
YES1	6.20 (5.55, 6.87)	6.31 (5.75, 6.78)	0.8	>0.9
PIK3CA	4.33 (4.11, 4.44)	4.31 (4.07, 4.49)	>0.9	>0.9
[1] Median (IQR)				

Extended Data Table 3c: Somatic & transcriptomic landscape of primary resistance to T-DM1

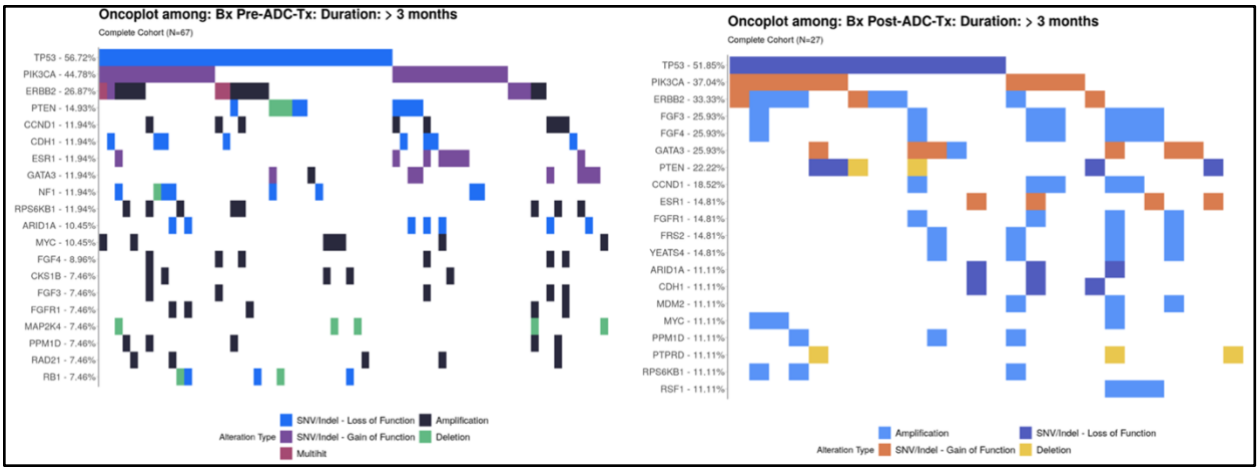

Extended Data Figure 1a: Oncoplot for somatic landscape in acquired resistance to T-DXd

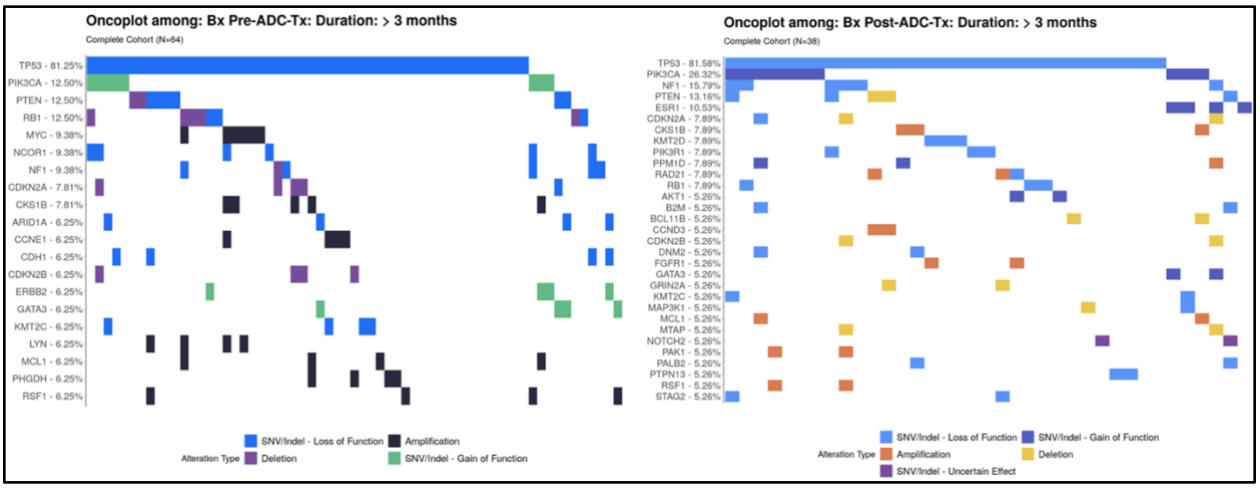

Extended Data Figure 1b: Oncoplot for somatic landscape in acquired resistance to SG

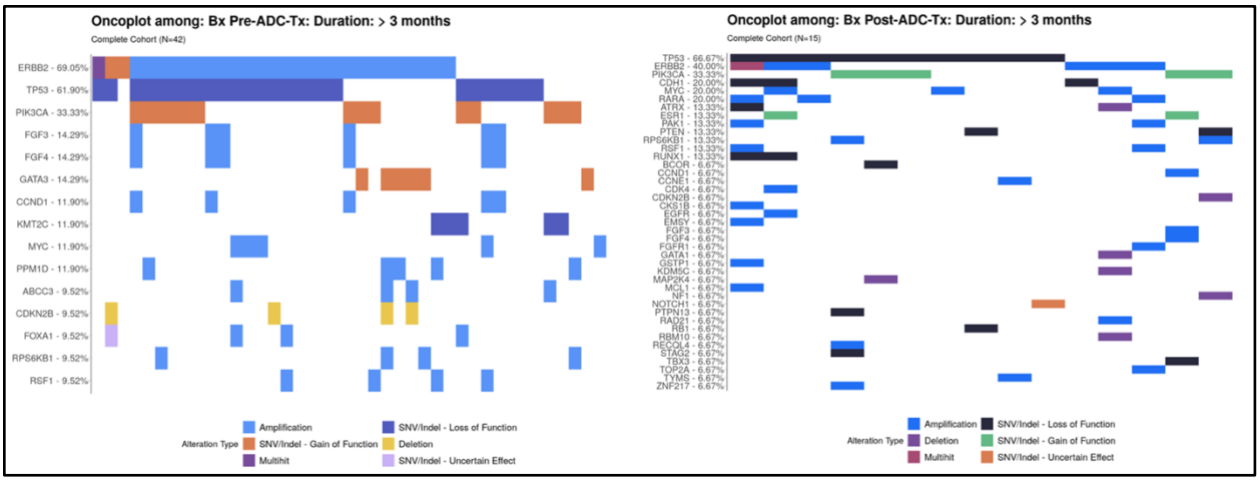

Extended Data Figure 1c: Oncoplot for somatic landscape in acquired resistance to T-DM1

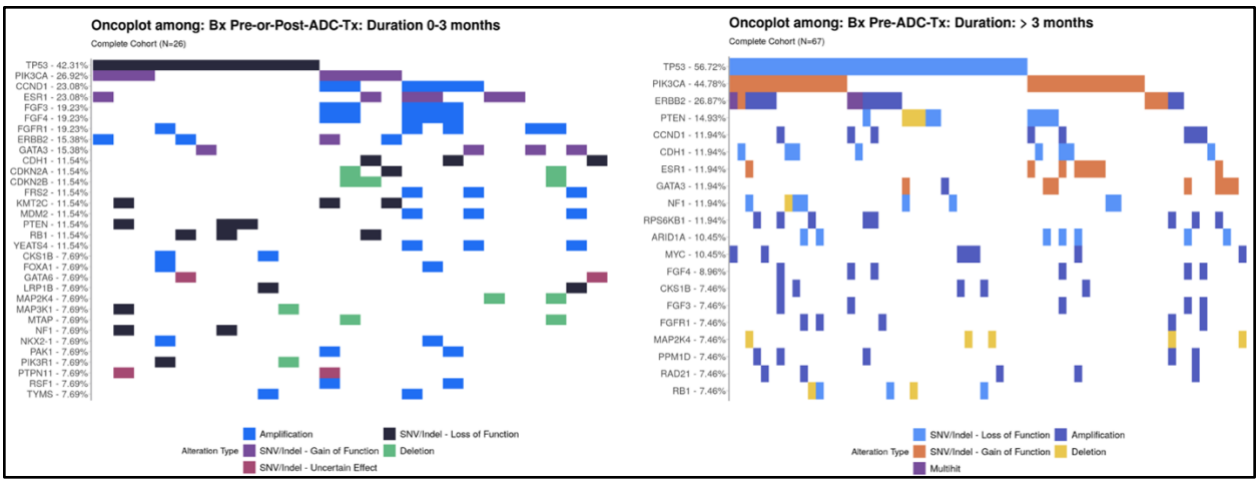

Extended Data Figure 2a: Oncoplot for somatic landscape in primary resistance to T-DXd

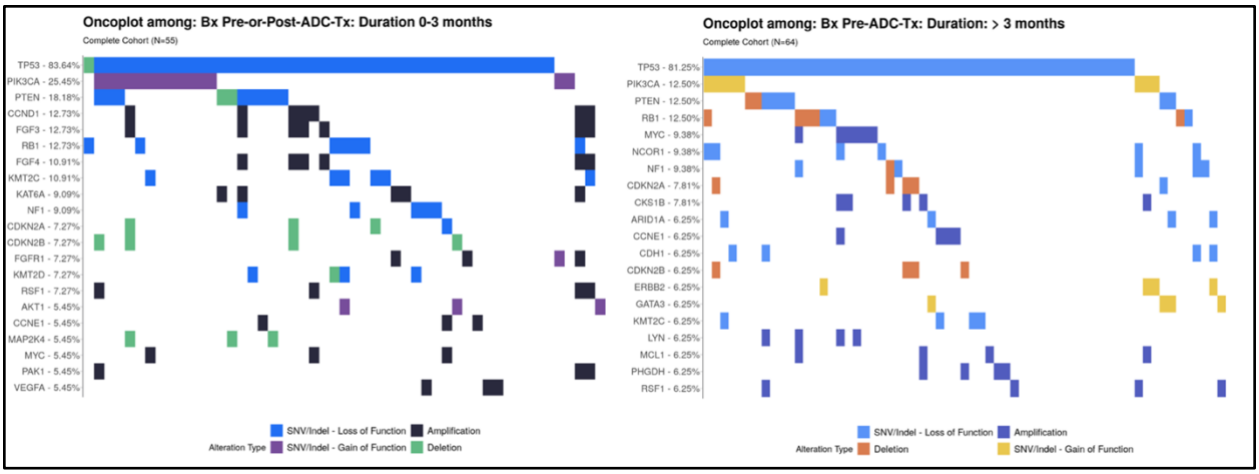

Extended Data Figure 2b: Oncoplot for somatic landscape in primary resistance to SG

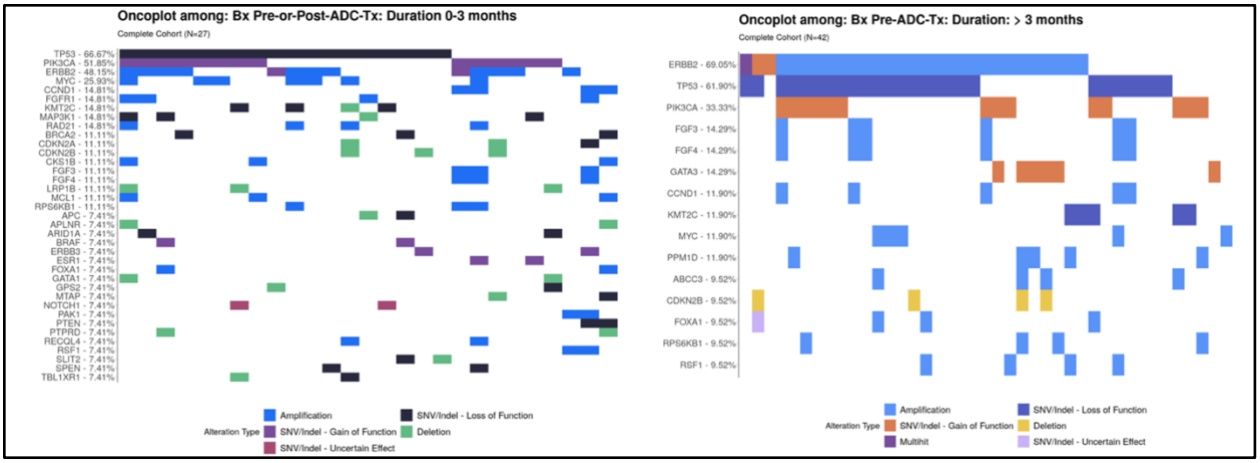

Extended Data Figure 2c: Oncoplot for somatic landscape in primary resistance to T-DM1

REFERENCES

1. Narayan, P. *et al.* FDA Approval Summary: Fam-Trastuzumab Deruxtecan-Nxki for the Treatment of Unresectable or Metastatic HER2-Positive Breast Cancer. *Clinical Cancer Research* **27**, 4478–4485 (2021).
2. Wedam, S. *et al.* FDA Approval Summary: Ado-Trastuzumab Emtansine for the Adjuvant Treatment of HER2-positive Early Breast Cancer. *Clinical Cancer Research* **26**, 4180–4185 (2020).
3. Wahby, S. *et al.* FDA Approval Summary: Accelerated Approval of Sacituzumab Govitecan-hziy for Third-line Treatment of Metastatic Triple-negative Breast Cancer. *Clinical Cancer Research* **27**, 1850–1854 (2021).
4. FDA approves datopotamab deruxtecan-dlnk for unresectable or metastatic, HR-positive, HER2-negative breast cancer. https://www.fda.gov/drugs/resources-information-approved-drugs/fda-approves-datopotamab-deruxtecan-dlnk-unresectable-or-metastatic-hr-positive-her2-negative-breast (2025).
5. Schipilliti, F. M. *et al.* Datopotamab deruxtecan: A novel antibody drug conjugate for triple-negative breast cancer. *Heliyon* **10**, e28385 (2024).
6. Kopp, A. *et al.* Antibody–Drug Conjugate Sacituzumab Govitecan Drives Efficient Tissue Penetration and Rapid Intracellular Drug Release. *Mol Cancer Ther* **22**, 102–111 (2023).
7. Hunter, F. W. *et al.* Mechanisms of resistance to trastuzumab emtansine (T-DM1) in HER2-positive breast cancer. *Br J Cancer* **122**, 603–612 (2020).
8. Chang, H. L., Schwettmann, B., McArthur, H. L. & Chan, I. S. Antibody-drug conjugates in breast cancer: overcoming resistance and boosting immune response. *Journal of Clinical Investigation* **133**, (2023).

9. García-Alonso, S., Ocaña, A. & Pandiella, A. Resistance to Antibody–Drug Conjugates. *Cancer Res* **78**, 2159–2165 (2018).

10. Khoury, R. *et al.* Mechanisms of Resistance to Antibody-Drug Conjugates. *Int J Mol Sci* **24**, 9674 (2023).

11. Baldassarre, T., Truesdell, P. & Craig, A. W. Endophilin A2 promotes HER2 internalization and sensitivity to trastuzumab-based therapy in HER2-positive breast cancers. *Breast Cancer Research* **19**, 110 (2017).

12. Chen, Y., Xu, Y., Shao, Z. & Yu, K. Resistance to antibody-drug conjugates in breast cancer: mechanisms and solutions. *Cancer Commun* **43**, 297–337 (2023).

13. Le Joncour, V. *et al.* A Novel Anti-HER2 Antibody–Drug Conjugate XMT-1522 for HER2-Positive Breast and Gastric Cancers Resistant to Trastuzumab Emtansine. *Mol Cancer Ther* **18**, 1721–1730 (2019).

14. Loganzo, F. *et al.* Tumor Cells Chronically Treated with a Trastuzumab–Maytansinoid Antibody–Drug Conjugate Develop Varied Resistance Mechanisms but Respond to Alternate Treatments. *Mol Cancer Ther* **14**, 952–963 (2015).

15. Li, G. *et al.* Mechanisms of Acquired Resistance to Trastuzumab Emtansine in Breast Cancer Cells. *Mol Cancer Ther* **17**, 1441–1453 (2018).

16. Coates, J. T. *et al.* Parallel Genomic Alterations of Antigen and Payload Targets Mediate Polyclonal Acquired Clinical Resistance to Sacituzumab Govitecan in Triple-Negative Breast Cancer. *Cancer Discov* **11**, 2436–2445 (2021).

17. Mosele, F. *et al.* Trastuzumab deruxtecan in metastatic breast cancer with variable HER2 expression: the phase 2 DAISY trial. *Nat Med* **29**, 2110–2120 (2023).

18. Nourieh, M., Vibert, R., Saint-Ghislain, M., Cyrta, J. & Vincent-Salomon, A. Next-generation sequencing in breast pathology: real impact on routine practice over a decade since its introduction. *Histopathology* **82**, 162–169 (2023).

19. Beaubier, N. *et al.* Clinical validation of the tempus xT next-generation targeted oncology sequencing assay. *Oncotarget* **10**, 2384–2396 (2019).

20. Beaubier, N. *et al.* Integrated genomic profiling expands clinical options for patients with cancer. *Nat Biotechnol* **37**, 1351–1360 (2019).

21. Tempus AI, Inc. Tempus xT Validation Summary. Tempus AI, Inc. Official Website. https://www.tempus.com/wp-content/uploads/2025/02/Tempus-xT_Validation.pdf?srsltid=AfmBOooNO158R3gZriB4zqqb0Kwvp8UyFnZXfnNAaB7EoLo7lpE9KnLU.

22. Michuda, J. *et al.* Validation of a Transcriptome-Based Assay for Classifying Cancers of Unknown Primary Origin. *Mol Diagn Ther* **27**, 499–511 (2023).

23. Tempus AI, Inc. Tempus xR Validation Summary. Tempus.com. Published May 2023. https://www.tempus.com/wp-content/uploads/2023/06/Tempus-xR_Validation.pdf.

24. Burris, H. A. *et al.* Phase II Study of the Antibody Drug Conjugate Trastuzumab-DM1 for the Treatment of Human Epidermal Growth Factor Receptor 2 (HER2) –Positive Breast Cancer After Prior HER2-Directed Therapy. *Journal of Clinical Oncology* **29**, 398–405 (2011).

25. Vance, G. H. *et al.* Genetic Heterogeneity in HER2 Testing in Breast Cancer: Panel Summary and Guidelines. *Arch Pathol Lab Med* **133**, 611–612 (2009).

26. Hanna, W. M. *et al.* HER2 in situ hybridization in breast cancer: clinical implications of polysomy 17 and genetic heterogeneity. *Modern Pathology* **27**, 4–18 (2014).

27. Lee, H. J. *et al.* HER2 Heterogeneity Affects Trastuzumab Responses and Survival in Patients With HER2-Positive Metastatic Breast Cancer. *Am J Clin Pathol* **142**, 755–766 (2014).

28. Allison, K. H., Dintzis, S. M. & Schmidt, R. A. Frequency of HER2 Heterogeneity by Fluorescence In Situ Hybridization According to CAP Expert Panel Recommendations. *Am J Clin Pathol* **136**, 864–871 (2011).

29. Hanna, W., Nofech-Mozes, S. & Kahn, H. J. Intratumoral Heterogeneity of HER2/neu in Breast Cancer?A Rare Event. *Breast J* **13**, 122–129 (2007).

30. Bartlett, A. I. *et al.* Heterogeneous HER2 Gene Amplification. *Am J Clin Pathol* **136**, 266–274 (2011).

31. Seol, H. *et al.* Intratumoral heterogeneity of HER2 gene amplification in breast cancer: its clinicopathological significance. *Modern Pathology* **25**, 938–948 (2012).

32. Filho, O. M. *et al.* Impact of HER2 Heterogeneity on Treatment Response of Early-Stage HER2-Positive Breast Cancer: Phase II Neoadjuvant Clinical Trial of T-DM1 Combined with Pertuzumab. *Cancer Discov* **11**, 2474–2487 (2021).

33. de Haas, S. *et al.* Abstract P6-07-09: Biomarker analysis from the neoadjuvant KRISTINE study in HER2-positive early breast cancer (EBC). *Cancer Res* **77**, P6-07-09-P6-07–09 (2017).

34. Sauveur, J. *et al.* Characterization of T-DM1-resistant breast cancer cells. *Pharmacol Res Perspect* **8**, (2020).

35. Loganzo, F., Sung, M. & Gerber, H.-P. Mechanisms of Resistance to Antibody–Drug Conjugates. *Mol Cancer Ther* **15**, 2825–2834 (2016).

36. Abelman, R. O. *et al.* Abstract 3888: TOP1 mutations mediate cross resistance to ADCs in metastatic breast cancer. *Cancer Res* **84**, 3888–3888 (2024).

37. Abelman, R. O. *et al.* TOP1 Mutations and Cross-Resistance to Antibody–Drug Conjugates in Patients with Metastatic Breast Cancer. *Clinical Cancer Research* OF1–OF9 (2025) doi:10.1158/1078-0432.CCR-24-2771.

38. Lee, J. *et al.* The DNA repair pathway as a therapeutic target to synergize with trastuzumab deruxtecan in HER2-targeted antibody–drug conjugate–resistant HER2-overexpressing breast cancer. *Journal of Experimental & Clinical Cancer Research* **43**, 236 (2024).

39. Mosele, M. F. *et al.* LBA1 Unraveling the mechanism of action and resistance to trastuzumab deruxtecan (T-DXd): Biomarker analyses from patients from DAISY trial. *Annals of Oncology* **33**, S123 (2022).

40. Shah, S. *et al.* Assessment of SLX4 Mutations in Hereditary Breast Cancers. *PLoS One* **8**, e66961 (2013).

41. Cardillo, T. M. *et al.* Predictive biomarkers for sacituzumab govitecan efficacy in Trop-2-expressing triple-negative breast cancer. *Oncotarget* **11**, 3849–3862 (2020).

42. Hamblett, K. J. *et al.* Effects of Drug Loading on the Antitumor Activity of a Monoclonal Antibody Drug Conjugate. *Clinical Cancer Research* **10**, 7063–7070 (2004).

43. Sun, X. *et al.* Effects of Drug–Antibody Ratio on Pharmacokinetics, Biodistribution, Efficacy, and Tolerability of Antibody–Maytansinoid Conjugates. *Bioconjug Chem* **28**, 1371–1381 (2017).

44. Yoder, N. C. *et al.* A Case Study Comparing Heterogeneous Lysine- and Site-Specific Cysteine-Conjugated Maytansinoid Antibody-Drug Conjugates (ADCs) Illustrates the Benefits of Lysine Conjugation. *Mol Pharm* **16**, 3926–3937 (2019).

45. Bai, C. *et al.* Site-Specific Conjugation of the Indolinobenzodiazepine DGN549 to Antibodies Affords Antibody–Drug Conjugates with an Improved Therapeutic Index as Compared with Lysine Conjugation. *Bioconjug Chem* **31**, 93–103 (2020).

46. Yu, M., Ocana, A. & Tannock, I. F. Reversal of ATP-binding cassette drug transporter activity to modulate chemoresistance: why has it failed to provide clinical benefit? *Cancer and Metastasis Reviews* **32**, 211–227 (2013).

47. Kovtun, Y. V. *et al.* Antibody-Maytansinoid Conjugates Designed to Bypass Multidrug Resistance. *Cancer Res* **70**, 2528–2537 (2010).

48. Chang, C.-H. *et al.* Combining ABCG2 Inhibitors with IMMU-132, an Anti–Trop-2 Antibody Conjugate of SN-38, Overcomes Resistance to SN-38 in Breast and Gastric Cancers. *Mol Cancer Ther* **15**, 1910–1919 (2016).

49. Cianfriglia, M. The biology of MDR1-P-glycoprotein (MDR1-Pgp) in designing functional antibody drug conjugates (ADCs): the experience of gemtuzumab ozogamicin. *Ann Ist Super Sanita* **49**, 150–68 (2013).

50. Takegawa, N. *et al.* DS-8201a, a new HER2-targeting antibody–drug conjugate incorporating a novel DNA topoisomerase I inhibitor, overcomes HER2-positive gastric cancer T-DM1 resistance. *Int J Cancer* **141**, 1682–1689 (2017).

51. Sledge Jr, G. W. *et al.* Mechanisms of Resistance to Trastuzumab Deruxtecan in Breast Cancer Elucidated by Multi-omic Molecular Profiling. in (San Antonio Breast Cancer Symposium 2024).

52. Bardia, A. *et al.* Genomic alterations in DNA damage response (DDR) genes in HR+/HER2- metastatic breast cancer (mBC) and impact on clinical efficacy with sacituzumab govitecan (SG): Biomarker results from TROPICS-02 study. *Journal of Clinical Oncology* **42**, 1075–1075 (2024).

53. Engebraaten, O. *et al.* RAB5A expression is a predictive biomarker for trastuzumab emtansine in breast cancer. *Nat Commun* **12**, 6427 (2021).